KTH Electrical Engineering

Iterative Road Grade Estimation for Heavy Duty Vehicle Control

PER SAHLHOLM

Licentiate Thesis
Stockholm, Sweden 2008

KTH School of Electrical Engineering
Automatic Control Lab
SE-100 44 Stockholm
SWEDEN

TRITA-EE 2008:056
ISSN 1653-5146
ISBN 978-91-7415-186-2

Akademisk avhandling som med tillstånd av Kungl Tekniska högskolan framlägges till offentlig granskning för avläggande av teknologie licentiatexamen i reglerteknik fredagen den 5 December 2008 kl 10.15 i sal V1, Kungl Tekniska högskolan, Teknikringen 76, Stockholm.

Tryck: Universitetsservice AB

Abstract

This thesis presents a new method for iterative road grade estimation based on sensors that are commonplace in modern heavy duty vehicles. Estimates from multiple passes of the same road segment are merged together to form a road grade map, that is improved each time the vehicle revisits an already traveled route. The estimation algorithm is discussed in detail together with its implementation and experimental evaluation on real vehicles.

An increasing need for goods and passenger transportation drives continuing worldwide growth in road transportation while environmental concerns, traffic safety issues, and cost efficiency are becoming more important. Advancements in microelectronics open the possibility to address these issues through new advanced driver assistance systems. Applications such as predictive cruise control, automated gearbox control, predictive front lighting control and hybrid vehicle state-of-charge control benefit from preview road grade information. Using global navigation satellite systems an exact vehicle position can be obtained. This enables stored maps to be used as a source of preview road grade information. The task of creating such maps is addressed herein by the proposal of a method where the vehicle itself estimates the road grade each time it travels along a road and stores the information for later use.

The presented road grade estimation method uses data from sensors that are standard equipment in heavy duty vehicles equipped with map-based advanced driver assistance systems. Measurements of the vehicle speed and the engine torque are combined with observations of the road altitude from a GPS receiver in a Kalman filter, to form a road grade estimate based on a system model. The noise covariance parameters of the filter are adjusted during gear shifts, braking and poor satellite coverage. The estimated error covariance of the road grade estimate is then used together with its absolute position to update a stored road grade map, which is based on all previous times the vehicle has passed the same location.

Highway driving trials detailed in the thesis demonstrate that the proposed method is capable of accurately estimating the road grade based on few road traversals. The performance of the estimator under conditions such as braking, gear shifting, and loss of satellite coverage is presented. The experimental results indicate that road grade estimates from the proposed method are accurate enough to be used in predictive vehicle control systems to enhance safety, efficiency, and driver comfort of heavy duty vehicles.

Acknowledgements

First I would like to thank my supervisor Karl Henrik Johansson for always providing enthusiasm and endless energy, it has been a great source of inspiration during this work. Even when you are on other side of the world you somehow manage to find time to comment on my drafts. Thanks also go to my co-supervisor during much of the research behind this thesis, Henrik Jansson. This project started with a real world problem, and you were vital in simplifying and dividing that problem into something manageable.

At Scania I have had three managers since the start of this work. I thank Michael Blackenfelt for hiring me as an engineer and then letting me switch jobs within the group shortly thereafter to begin this project. I thank Nils-Gunnar Vågstedt for taking over the lead and managing the project. Your optimism and wide network of contacts have opened many doors. Many thanks also go to my current manager Tony Sandberg for helping me find time to focus on getting this book written.

Thanks to Maria Ivarsson for the cooperation we have had in this project, proofreading parts of the manuscript, and all the invaluable help you and Erik Hellström have given with collecting experimental data. Thanks for reading and commenting on parts of the manuscript also go to Benjamin Bruhn and my father Ewert Bengtsson. Many thanks also to my mother Brita Nederman for caring for Vilgot when I felt I needed a few extra hours to finish the thesis.

I would like to thank Lars Nielsen for your valuable feedback in the project steering group. Thanks also go to Anders Jensen and all others who have attended the reference group meetings and supported the project.

All my colleagues at both Scania and KTH deserve great thanks for providing such an inspiring and positive work environment.

The research presented in this thesis is jointly financed by the Intelligent Vehicle Safety System (IVSS) programme, a part of the Program Board for Automotive Research, and by Scania CV AB. The financial support is appreciated.

Finally, extra special thanks to Anna and Vilgot for being what really matters in life.

Sincerely

Per

Acronyms

ADAS	Advanced driver assistance systems
CAN	Controller area network
CEP	Circle error probable
EKF	Extended Kalman filter
GPS	Global positioning system
HDV	Heavy duty vehicle
RMSE	Root mean square error

Contents

Chapter 1

Introduction

Modern heavy duty vehicles (HDVs) employ several electronic control systems that utilize information about the vehicle and its environment to increase efficiency, safety and comfort. The road grade is a key variable that heavily influences the longitudinal dynamics and energy flow in a HDV. This thesis describes a method by which the grade of roads traveled frequently can be estimated without the need for any extra equipment beyond what is already commonly available in modern HDVs. The first section of this chapter provides a motivation for the project by describing look ahead vehicle control. This is followed by a brief discussion about road grade estimation, before the problem statement for the thesis is given. Section 1.4 lists the publications forming the basis for the thesis, and the final section gives an outline of the rest of the thesis.

1.1 Advanced Driver Assistance Systems

The economic development of the world is driving a continuing increase in the demand for goods transportation. Environmental concerns together with competitive pressure to increase efficiency make any technology that shows a potential for reductions in energy consumption highly interesting. The increase in road transportation also intensifies the demand for new safety systems, to protect road users in increasingly complex traffic environments. One area that shows promise to both improve road safety and reduce energy consumption in vehicles is electronic advanced driver assistance systems (ADAS). Sensors, which are a part of many such systems, help the driver by improving the total perception of the environment. In the case of look ahead systems, a map with stored information is used to extend the perception horizon beyond what either the driver or conventional on-board sensors can see. Actuators connected to ADAS improve vehicle control by acting in situations where the driver is unable to do so. In map based look ahead systems the automatic action can be based on information that the driver will only be able to get at a later time.

An increasing number of vehicle control systems now utilize stored information

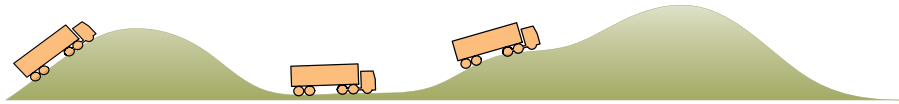

Figure 1.1: HDVs traveling on a hilly road. At the position of the leftmost vehicle, it is advantageous to lower the speed to take full advantage of the upcoming downhill road segment. In the second position the overall fuel economy can be improved by increasing the speed before the steep part of the hill is reached. In the third position it is important to maintain the driving torque, to avoid costly loss of turbo pressure when entering the continued ascent.

from a map, to aid the driver in piloting the truck in a safe and economical manner. Examples of map attributes that are commonly used are speed restrictions, road class, road curvature and road grade. Knowledge of the current and future road grade can be used in engine and gearbox control systems to help meet the instantaneous power demand while keeping fuel consumption and environmental impact as low as possible.

The HDV in Figure 1.1 will speed up when going down one hill, and loose speed when climbing the next one. If the road grade for the kilometer or so directly ahead of the vehicle is known, it is possible to automatically adjust the speed in advance of up- and downhill road segments and thus conserve fuel without increasing trip time. The preview road grade information can also be utilized when determining if a gearshift should be performed or the state of some energy buffer changed. Furthermore the brake management system could use the road grade information to determine the highest allowable speed when going down a hill. Thus waste heat generation in excess of the system's ability to release it can be avoided. This in turn ensures that the vehicle retains emergency stopping power, a clear safety benefit.

Road grade maps of sufficient accuracy to support automatic vehicle control systems are currently not widely available. Commercial efforts to create such maps are underway, but access to them will most certainly be associated with some cost. HDVs commonly travel the same routes frequently, and are thus ideally suited to be their own probes and estimate the road grade for the small subset of all roads that are relevant for a particular vehicle.

1.2 Road Grade Estimation

Information about the current state of the vehicle is commonly acquired through various on-board sensors. Information about factors that will influence the vehicle in the future cannot generally be sensed directly. However, a map with stored attributes can provide the required look-ahead information and enable new control algorithms to improve overall vehicle performance. An attribute recorded at the current position in one run along the can be used as look ahead information in the



Figure 1.2: The proposed road grade estimation algorithm has been tested on highway E4 between Södertälje and Nyköping, using three types of HDVs. (Photographs courtesy of Scania CV AB)

next run. In order to use the map the vehicle needs to be able to position itself, this is most commonly solved by installing a satellite navigation system receiver. Fortunately, those are both cheap and commonplace nowadays.

One road attribute which lends itself to estimation using standard HDV onboard sensors and recording in a map is the road grade. If a road is driven frequently, many estimates of the road grade can be obtained, and these can be used to increase confidence in the created map. This thesis proposes such a method for road grade estimation and investigates its performance when applied to real measurements. The method has been evaluated experimentally using the three types of HDVs shown in Figure 1.2.

The final grade estimate created by the method, based on six experiments on a 15 km test segment of the southbound highway E4 south of Södertälje is shown together with a reference road grade profile in Figure 1.3. The proposed method is able to estimate the road grade in the presented experiments with a bias of $-0.10\,\%$ grade, and with an approximately normal error distribution with a mean standard deviation around the bias of $0.14\,\%$ grade.

1.3 Problem Formulation

The problem studied in this thesis is how to estimate the road grade of roads that are frequently traveled by a HDV, based on sensors that are part of the standard vehicle equipment. A HDV climbing a hill with a road grade α, and the most important forces affecting the vehicle, are shown in Figure 1.4. The vehicle is described by a dynamic model f_v for its longitudinal movement, that links the road grade to the engine torque and the absolute altitude. The road is modeled with one state for the altitude, whose dynamics are described by f_z, and one for the road

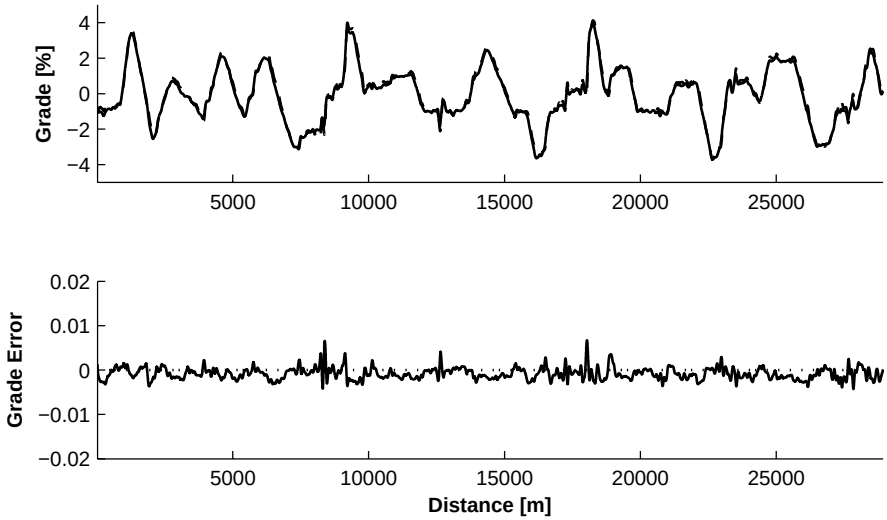

Figure 1.3: The first part shows the estimated road grade profile for the southbound direction on highway E4 south of Södertälje, based on six road experiments with three different vehicles (solid), compared to a reference road grade profile (dashed). The second part shows the error in the estimated grade.

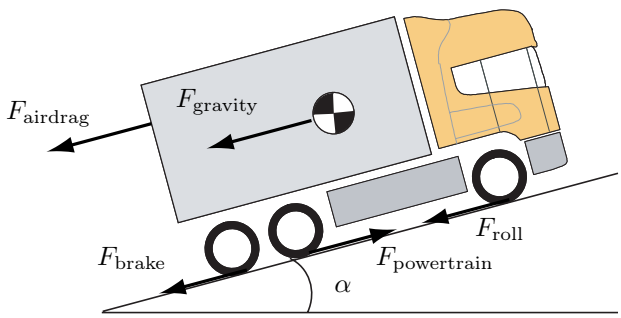

Figure 1.4: A HDV traveling on a road is affected by forces from its powertrain, rolling resistance, air resistance, gravity and possibly its brake system. The influence of gravity depends on the road grade α.

grade. The total system model is

$$\begin{aligned} \frac{dv}{ds} &= f_v(v, \alpha, T_e) \\ \frac{dz}{ds} &= f_z(\alpha) \\ \frac{d\alpha}{ds} &= 0 \end{aligned} \tag{1.1}$$

where s is the distance along the road, v is the vehicle speed, α is the road grade, T_e is the engine torque, and z is the absolute altitude of the vehicle.

The vehicle speed and engine torque are available in the vehicle control network. The altitude can be determined from a GPS receiver. The GPS receiver also reports the number of tracked satellites, this signal is used to assess the accuracy of the altitude signal. The vehicle dynamics model f_v depends on which gear is engaged, if any. This information is obtained by sensing the current gear and if a gearshift is in progress. When the vehicle is braking the dynamics will be radically different than otherwise. Since the brake force F_{brake} is not available for measurement the road grade estimation is done with only a status signal indicating if braking is taking place. Since the task is to estimate roads that are traveled frequently, a position log from the GPS is included to enable many estimates of the road grade to be merged. Finally the GPS receiver vehicle speed signal is recorded and used to calibrate the in-vehicle speed sensor.

The system model and sensor information are used together to create the road grade estimator shown in Figure 1.5. The estimator uses a Kalman filter with the time varying system model to obtain a first grade estimate. Rauch-Tung-Striebel smoothing is then applied to increase the measurement information used and avoid filter lag. The smoothed estimate is then used to update a stored map based on the relative reliability of the latest estimate and the already stored data.

The problem that is solved in this thesis is how to use sensor signals already available in many HDVs to iteratively create road grade maps based on all the sensor information available from many runs along the same roads.

1.4 Contributions

This thesis presents a method for road grade estimation based on the following publications:

- **P. Sahlholm, H. Jansson, E. Kozica, and K. H. Johansson**, A Sensor and Data Fusion Algorithm for Road Grade Estimation. In proceedings of Fifth IFAC Symposium on Advances in Automotive Control, Monterey Coast CA, USA, 2007.
- **P. Sahlholm, H. Jansson, and K. H. Johansson.** Road Grade Estimation Results Using Sensor and Data Fusion. In proceedings of 14th World Congress on Intelligent Transport Systems, Beijing, China, 2007.

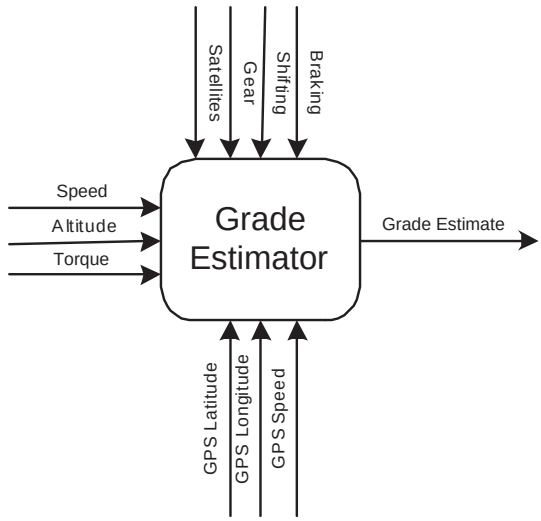

Figure 1.5: The studied problem is how to estimate the road grade based on sensor information from a standard HDV. The presented estimator uses a number of input signals to iteratively estimate the road grade based on many runs along a given road.

- **P. Sahlholm, and K. H. Johansson.** Road Grade Estimation for Look-Ahead Vehicle Control. In proceedings of 17th IFAC World Congress, Seoul, Korea, 2008

The first paper, presented at the Fifth IFAC Symposium on Advances in Automotive Control in August of 2007, outlines the basic ideas of the methods and initial grade estimation results. The second publication presented at the 14th World Congress on Intelligent Transport Systems later in the fall of 2007 incorporates results from using additional data with the method. The most recent contribution, presented at the 17th IFAC World Congress in July 2008, gives a deeper analysis of the grade estimator. In that paper the possibility of using a linear instead of a non-linear vehicle model is also investigated.

The key idea behind the road grade estimation method has been patented, and is described in the Swedish patent:

- **P. Sahlholm, H. Jansson, E. Kozica**, Metod och anordning för estimering av lutningen för ett underlag på vilket ett fordon färdas. Swedish patent no. 530 728 C2, published Aug. 26, 2008.

A leading motivation for estimating the road grade is the possibility of using a known future grade profile to plan an efficient vehicle speed trajectory. The negative effects of errors in the assumed road grade profile are explored in:

- **P. Sahlholm** Improved Heavy Duty Vehicle Performance Through the Use of 3D Map Data. In proceedings of 15th World Congress on Intelligent Transport Systems, New York, NY, USA, 2008.

1.5 Outline

The rest of this thesis is organized as follows. Chapter 2 includes a motivation for the project as well as background information and references regarding road grade mapping, look ahead vehicle control and the GPS. The system model used in the road grade estimator is developed in Chapter 3. Chapter 4 describes the filtering and data fusion steps taken to arrive at the final road grade map. Practical applicability has been a primary concern in the development of the method, and an extensive account for the experimental results achieved is given in Chapter 5. The thesis is concluded, and a number of areas of interest for future improvement and expansion are identified in Chapter 6.

Chapter 2

Background

The need for accurate digitized information about the road grade has emerged recently as the evolution of embedded electronics has made HDV control units powerful enough to take such information into account in real-time. When the control algorithms are extended from considering only the local road grade to also include the upcoming grade profile it becomes impractical to sense the data as it is needed. The situation calls for a digital road map that includes sufficient information about the road grade. As more than one system that uses look ahead information is introduced in the vehicle, a need also arises for a some way of distributing the look ahead information from where it is stored to all the locations in the distributed vehicle control system where it is needed.

This chapter starts off with a description of previous work in the area of road grade estimation and map building. It then continues with an overview of the state of the art in look ahead ahead vehicle control, with a bias towards issues of relevance for HDVs. The needs of emerging look ahead control systems serve as a motivation for studying road grade map generation. The next section investigates the road grade requirements set forth by a specific application; energy optimal predictive cruise control. Next follows a discussion on the sensors used in the proposed method. A summary concludes the chapter.

2.1 Road Grade Maps

A multitude of methods for estimating the road grade can be found in the literature. In many cases the instantaneous road grade at the vehicle position is the primary objective in the estimation, but there are also various methods intended for mapping and survey applications. As a general rule methods for estimation of the instantaneous road grade in production vehicles includes system cost as an important parameter. Contributions focused on mapping applications generally utilize expensive hardware, that enables accurate results in a single pass over the road. The approach described herein, where many measurement from low-cost sensors are merged into a road grade map is quite rare.

The term road grade will be used in this work to refer to the rate of change in the road surface altitude along the direction of travel for the road. In the mathematical models the road grade is expressed as an angle between the roadway and the horizontal plane, measured in radians. It is common, e.g. on road signs to express road grade in terms of percent. This generally refers to an altitude difference divided by a corresponding traveled distance. It is sometimes ambiguous whether the traveled distance is measured along the incline, or if the distance along a virtual horizontal reference plane should be used. The difference in practice is very small, it does not reach 1 % of the road grade until a grade of approximately 14 %. In this work all road grade results are presented as percent, calculated as the ratio of altitude change divided by the covered distance in the horizontal plane. This quantity can be determined from the road plane angle relative to the horizontal plane as

$$\alpha_{\%} = 100 \text{ atan } \alpha_{radians}$$

Expressing changes or intervals of a quantity expressed with the unit % is somewhat delicate. One have to make the distinction between a 5 % change from a grade of 2.0 % to 2.1 % and a 5 percentage points change from 2.0 % to 7.0 %. To make this clear the term "% grade" will be used as shorthand whenever the intended meaning is a change denoted as percentage points of road grade.

One common approach for estimation of the instantaneous road grade is to use a sensor to directly measure the grade. A direct road grade sensor for automotive use is described in a patent application filed as early as 1971 by (Gaeke, 1973). More recent contributions often employ GPS receivers of various kinds to obtain road grade estimates. In (Bae *et al.*, 2001) a grade estimation method based on a GPS receiver with 3D velocity output is compared to one using a two-antenna GPS. The 3D velocity signal is used to calculate the grade as the ratio of the vertical and horizontal velocities, while the two antenna solution directly gives the grade as the height difference between the measurement points. The GPS receiver employed is a high performance model, and satellite reception is flawless during the entire test segment. Thanks to the high quality grade estimate a precise determination of the vehicle mass is possible through the use of a vehicle model similar to the one used in this thesis. Another effort based on high precision GPS equipment is described in (Han and Rizos, 1999), where a road in Australia has been surveyed using geodesy GPS receivers with stationary base stations for improved accuracy. A spatial Kalman filter with height and road grade states is used to post-process the data. Both these methods rely heavily on the existence of a high quality GPS signal, something that is not always available. Additionally, neither of the approaches is believed to work particularly well with the low cost GPS receivers that can be anticipated to be standard equipment in road vehicle in the coming few years.

The idea of using vehicle sensor information in combination with a longitudinal road model to find the road grade has been explored in (Lingman and Schmidtbauer, 2001), where a Kalman filter is used to process a measured or estimated propulsion force or estimated retardation force and a measured velocity into a road grade estimate. A similar method, where the grade is estimated using a "recursive least

squares" method based on a simple motion model has been suggested by (Vahidi *et al.*, 2005).

On-line road grade estimation based on accelerometers, calculated driveline torque and a vehicle model, or other on board sensors is state-of-the-art in today's vehicles. These methods have the advantage of not needing any external signal, such as the GPS, but hence don't provide the extra bias compensation or easy inclusion of data from multiple runs along the road. They are generally used to obtain data to support automatic gearboxes and other systems that currently use road grade information. One proposal, together with an up to date survey about common methods, can be found in (Fathy *et al.*, 2008)

The idea of automatic creation of road maps from GPS traces has been described in a few places. An interesting approach based on position logs from many runs along a road, using consumer grade GPS receivers, is described in (Schroedl *et al.*, 2004). Another automatic road map generation approach, based on more expensive DGPS receivers, is detailed in (Brüntrup *et al.*, 2005). The emphasis in this project is on the data mining methods being applied, and on achieving lane-level accuracy in the generated maps. Both these contributions treat 2D-maps without road grade information. They also do not explore the possibility to use a vehicle model and on-board sensors to improve accuracy.

Use of high resolution specialized measuring equipment is also described in (Noyer *et al.*, 2008), where an attempt is made at defining a map production method with curve clothoid identification for a lane-level accurate map. The roads to be mapped have to be driven by the probe vehicle, but there is no need to interfere with the regular flow of traffic, as there is with classical surveying methods. The aim of the method is to produce a map with an accuracy one order of magnitude better than current street maps for navigation purposes, i.e. around one meter. The road grade is currently not treated by this method.

A research group in Germany is developing a self-learning route memory, that records vehicle state and driving events along frequently traveled roads. The system described aims to automatically identify route conditions accurately enough to be used in look ahead vehicle control applications such as predictive powertrain control for hybrid electric vehicles. The work has most recently been described in (Carlsson *et al.*, 2008), where a prototype implementation of the route memory is detailed. In this work significant attention is directed towards practical issues such as data storage requirements for different attributes, rather than the identification of attribute values, such as the road grade.

The iterative road grade estimation scheme described in this thesis was first described in (Sahlholm *et al.*, 2007b). Initial data from the highway experiments was presented in (Sahlholm *et al.*, 2007a). Further developments to the method, and a more detailed study of the benefits of merging data from multiple experiments was given in (Sahlholm *et al.*, 2008). This most recent paper also includes the linearized version of the system model.

The current major suppliers of road maps for navigation devices make up a potential source for digital maps with road grade information. The currently delivered

maps do not contain road grade or altitude information accurate enough to be used in vehicle control. However, the major companies in the field already have numerous measurement vehicles in the field, as well as a built up infrastructure for map production based on collected data. Relatively simple equipment upgrades to the measurement vehicles should enable road grade data to be included in the products. Plans to provide a compact low cost navigation system without a user interface, with only map attributes relevant for ADAS have recently been announced by one of the manufacturers (NAVTEQ Press Release, 2008).

It is apparent that the idea of using vehicle sensors and a model for the vehicle and road is not new. Solutions based on this idea have been implemented using a number of different methods, to reach various design goals. GPS receivers of varying quality are used in a number of methods for road map generation. What is new in this thesis is the particular method of combining the vehicle sensors and a GPS to create a road grade map based on many runs along a particular road segment.

2.2 Look Ahead Vehicle Control

The emerging availability of low cost high accuracy GPS receivers together with enhanced computational capabilities of embedded control systems and increased storage capacity has opened up new possibilities in vehicle control. Absolute global positioning combined with a map enables the vehicle to predict where it is going next, and exercise control actions based on this assumption. Many different types of attributes can be utilized in this way to the enhance vehicle safety and efficiency, but for HDV the road grade is the most important one.

Vehicle functions intended to support the driver, realized through electronic sensors, actuators and control units are usually referred to as ADAS. A multitude of such systems that utilize look ahead have been showcased in the last few years, but only a few have yet entered production. This section describes how ADAS benefit from access to electronic maps, and outlines main application areas where look ahead road grade information improves existing, or enables new, functionality. The systems covered are

- Speed Control for Energy Efficiency
- Hybrid Vehicle Control
- Control of Auxiliary Units
- Gearbox Control
- Adaptive Front Lighting Control
- Overtaking Assistance

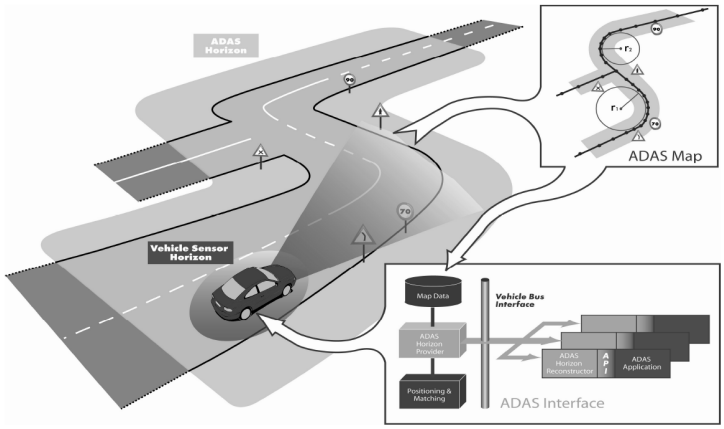

Figure 2.1: Illustration of an ADAS horizon with a number of physical and legal attributes. (Illustration courtesy of the PReVENT project)

There are already many more examples of imaginative ways of using look ahead road information, and more will undoubtedly follow once such information becomes universally available. These applications described here have been chosen for their relevance to HDVs and/or dependence on road grade information.

2.2.1 ADAS Horizon

A crucial part of a look ahead control system is the ability to extract the interesting part of a large map. The map is generally kept on a mass storage device, in some format that allows for fast searching based on geographical coordinates. As the vehicle moves a digital model of the surrounding road network with its associated attributes needs to be constructed. This model is commonly referred to as the ADAS horizon. Figure 2.1 shows an example ADAS horizon with both physical and legal attributes. The desired application places varying demands on the selection of ADAS horizon attributes, their accuracy, and the horizon size. In some applications one is only interested in the vehicle's most probable path, in others the entire horizon is taken into account. The most probable path based road network attributes such as road class and turn angles is shown in Figure 2.2.

To enable multiple look ahead applications in a distributed control system to use a single map data source there needs to be a method for transferring the ADAS horizon to different control units on the vehicle communication network. The ADASIS forum is a joint effort by slightly more than 30 ADAS oems, map suppliers and vehicle manufacturers to create a common solution for how to accomplish this. The ADASIS forum has developed a proposed standard for both the representation of attributes in the ADAS horizon and the transmission of these attributes over vehi-

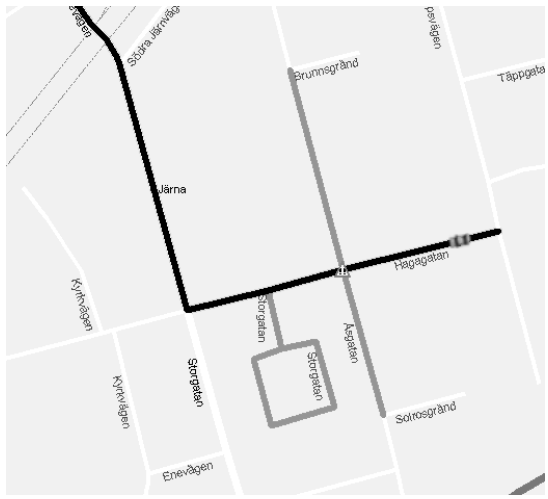

Figure 2.2: The ADAS horizon road network ahead of the car is shown in grey, and the most probable path is black. The vehicle is located in the middle right of the figure, heading left and soon to encounter an intersection, highlighted by a small warning sign. (Illustration courtesy of Navteq)

cle communications networks. These efforts started in 2001, and there is currently a fully functional proposal available. The most recent results from the forum can be found in (Ress *et al.*, 2008).

2.2.2 Speed Control for Energy Efficiency

When a highway contains segments with an uphill grade so steep that a vehicle cannot maintain the desired speed, or a downhill grade so steep that overspeeding will occur unless the brake system is used, there is a potential for decreasing the fuel consumption compared to a standard cruise controller, with unchanged trip time. This has been explored for example in (Hellström, 2007; Hellström *et al.*, 2007; Fröberg, 2008; Terwen *et al.*, 2004). To achieve a reduction in the fuel consumption it is necessary to lower the vehicle speed over hill crests and increase it ahead of steep uphill segments. Thus the number of steep hill segments as well as the traffic load of the road affect the fuel consumption gain that can be achieved.

Furthermore, road grade data of sufficient accuracy must be present for the highways where the vehicle will operate. The quality of the grade data needs to be high, so that the vehicle velocity can be predicted over a long enough distance. Field tests have shown that averaged single frequency GPS based measurements from a few runs along the road give sufficient precision to realize fuel savings in actual driving. The most crucial information needed by the optimization algorithm

is whether the vehicle will loose speed uphill despite running at full throttle or gain speed without fuel injection when going downhill. Not knowing the exact rate of the speed increase or decrease will reduce the possible savings due to the extra margins needed before action can be taken, but the principle of operation can remain largely unchanged. For typical long haulage HDVs the most interesting range of road grades will be 0% – 2% either up- or downhill.

2.2.3 Hybrid Vehicle Control

In hybrid electric vehicles one of the most challenging control objectives is to keep the state of charge of the energy buffer from hitting the boundaries of its operating range. In order to minimize energy consumption it is necessary to empty the buffer ahead of driving events that will generate surplus energy, such as braking or driving in steep downhill grades. On the other hand, driveability will generally suffer if the energy buffer happens to be empty when an event that requires maximum power output occurs. Since the problem of determining the optimal state of charge for the energy buffer at every point along the route depends on the power demands ahead of, as well as behind, the vehicle it seems natural to use some type of look ahead information. The road grade is one factor that influences the power demands of a hybrid electric vehicle, but the velocity profile is often of equal or higher importance. Much of the energy consumption gains using hybrid technology come from regenerative braking in city driving scenarios. Numerous solutions to how to utilize advance knowledge of both the road grade and anticipated velocity profile have been proposed in the literature. In (Johannesson, 2006) various predictive control strategies based on stochastic models of the road grade and velocity profiles for a hybrid electric passenger car in city traffic are evaluated. The work is extended further in (Johannesson and Egardt, 2007). A current and instructive survey of results obtained by route optimized control of hybrid electric vehicles, both passenger cars and HDVs, can be found in (Gonder, 2008), while a wider survey of the current state of energy buffer management research for hybrid electric vehicles is available in (Salmasi, 2007). A self learning system that identifies the power demands for various segments of a commuting route through many repeated measurements is described in (Ichikawa *et al.*, 2004).

2.2.4 Control of Auxiliary Units

A HDV contains a number of auxiliary units such as an electric generator, a power steering pump, a water pump, a cooling fan, an air compressor, an oil pump, and sometimes an air conditioning unit. A common trait of these is that they generally operate with some kind of energy buffer. As an example the electric generator charges a battery, and the power steering pump maintains pressure in the power steering system. For short periods of time the battery could potentially be used to power the electric system without the help of the generator, and the power steering pump might not need to run at full throttle when going straight. Advance

knowledge of the near future energy needs of auxiliary systems, combined with state information about their energy buffers, and improved auxiliary units that can be turned on and off enable look ahead control strategies to be used in pursuit of maximum energy efficiency. Similarly to the speed control case the units can be used to charge the buffers when there is an energy surplus available. The potential for energy savings from using more controllable auxiliaries is explored in (Pettersson and Johansson, 2006).

2.2.5 Gearbox Control

Automatic gearboxes stand to benefit considerably from advance knowledge of the upcoming road grade. Performing a gear shift takes some time, especially with the automated manual gearboxes that are commonplace in HDVs. During this time the turbo pressure is lost in the engine, and the vehicle slows down rapidly due to the absence of a driving torque. If the vehicle is near the top of the hill the gearshift can often be avoided, if the grade profile is known. Unnecessary downshifts near the end of uphill road segments are a well known annoyance to truck drivers using automatic gearboxes. Additionally, the shifting strategy and choice of starting gear can be improved in many other cases using reliable stored road grade information.

2.2.6 Safety and Comfort Systems

Two examples of look ahead systems that need road grade information, but focus on safety and driver comfort rather than energy efficiency, are adaptive front lighting control and overtaking assistance. The basic idea of front lighting control is that the center of the light beam should always be where the driver wants to look. In curves the headlamps then have to be angled sideways, and when the road grade changes the beams need to be adjusted up or down. With look ahead information about the 3D road profile, and full position state information about the vehicle, fully controllable headlamps can be directed to center on a specific point on the road, as described in e.g. (Löwenau *et al.*, 2000) and (Lauffenburger *et al.*, 2007).

The more passenger car focused overtaking assistance has been described as a utility to inform the driver of when it is unsafe to pass vehicles in front, and how far it is until the next location where there may be an overtaking opportunity (Löwenau *et al.*, 2006). In this application the road grade is of importance both to judge the visibility distance at any given point, and to determine the maximum relative acceleration available. The acceleration in turn determines the time required to pass the preceding vehicle.

2.3 Road Grade Requirements

The road grade information available in the vehicle will of course never be completely accurate. The effects of errors in the road grade depends on the system where the information is used. If the actual road grade profile does not match

the assumed profile when an optimal speed profile is calculated the control action that results will not remain optimal. To illustrate the effect of moderate errors in the road grade on optimal speed control a Monte Carlo simulation is made for a slightly perturbed simple road profile where the optimal speed trajectory is known for the nominal case. The results described in this section have previously appeared in (Sahlholm, 2008).

The tested road grade error model is based on a filtered white noise signal. A second order low-pass filter has been applied to a white noise sequence to obtain a time varying error signal with zero mean but mainly low frequency components. The resulting vertical error around the critical point of the nominal road profile is essentially zero mean normally distributed with $\sigma = 0.66$ m. The resulting road profiles are shown in Figure 2.3.

The energy consumption numbers for two different speed profiles are calculated in the analysis. The reference speed profile is one that would result from a standard vehicle cruise controller. This means that as long as a torque contribution from the engine is required in order to maintain a speed of at least 85 km/h the appropriate torque is applied. If gravity accelerates the vehicle above this speed, fueling is cut and the vehicle is allowed to accelerate. The brake system is used to ensure that the vehicle never exceeds 90 km/h. The cruise controller speed strategy results when applied to the test roads are shown as a solid line in Figure 2.4.

The second speed profile is based on the optimality results in (Fröberg, 2008). The allowable speed range is between 80 km/h and 90 km/h, with a set speed for level road segments of 85 km/h. There is also a requirement that fuel must not be saved by lowering the average speed. To achieve this an extra cost corresponding to the energy required to make up any lost time after the downhill segment is added to the end result. The resulting strategy involves cutting off fueling at the exact moment that will give a speed of 80 km/h when the vehicle reaches the point on the hill where it will start to accelerate solely under the influence of gravity. This point will be referred to as the *critical point*. The results of the second speed strategy applied to the perturbed roads are shown Figure 2.4. On level road the coasting deceleration distance for the test vehicle from 85 km/h to 80 km/h is about 170 m. On a gradually steeper hill the distance can be much longer, on the nominal test road it is 320 m.

The realized energy savings for each disturbed road profile divided by the nominal energy savings were investigated based on the vertical error at the critical point of the nominal road profile. The results are shown in Figure 2.5. The ratio of realized to potential energy savings is essentially 1 for small vertical errors. For negative errors (the disturbed road has descended further than the reference road) the realized energy savings decreases almost linearly. When the disturbance causes a vertical error of -1 m approximately 75% of the nominal energy savings are realized. This effect can intuitively be attributed to the fact that the vehicle does not slow down enough to take full advantage of the downhill grade.

For positive errors (the disturbed road has descended less than the reference road) the effects are less severe. The realized energy savings are essentially identical

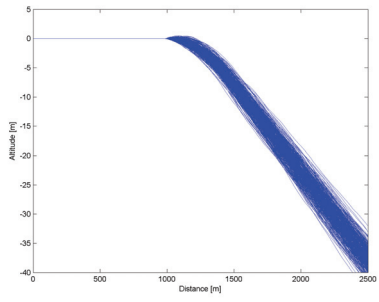

Figure 2.3: Road altitude as a function of distance for the 500 test road profiles generated by application of a filtered gaussian bias to the nominal road grade from the point (983 m) where the two speed strategies start to differ.

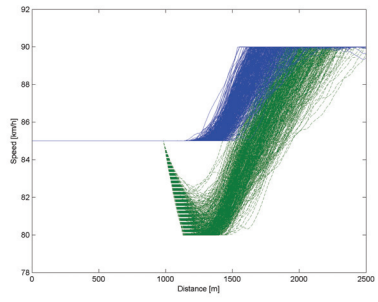

Figure 2.4: Speed profiles resulting from the randomly disturbed road grade profiles. Results from the cruise control are shown as solid lines, and results from the optimal control are dashed.

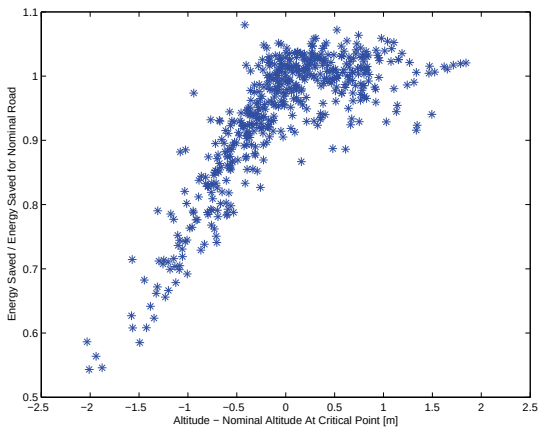

Figure 2.5: Results from the random process grade bias experiment. The ratio of energy saved when driving a modified road to energy saved when driving the reference road is shown against the magnitude of the altitude error at the nominal critical point. A negative altitude error causes the mean realizable energy savings to decrease almost linearly to about 60 % for an error of −1.6 m. Positive altitude errors have no mean effect on the energy savings, the average ratio is close to 1 for the investigated range of positive errors.

to the optimal case. In these cases the vehicle slows down to 80 km/h before the critical point, and then maintains that speed using the engine. The lost time penalty applied is not severe enough to cause an increase in the total energy cost.

2.4 Sensors

An important property of the presented road grade estimation method is that it only relies on sensors that are commonplace in HDVs, and that will most certainly be available in vehicles that are to be equipped with map based predictive control. It is thus suitable for deployment in a large number of vehicles, without significant hardware costs, given that the computational and data storage requirements can be met by the vehicle platform. The restriction of creating a method based on existing mass market sensors limit the accuracy that can be expected from the input data. The grade estimator is thus constructed to use many measurements from the same location in the map creation process.

2.4.1 Driveline Sensors

The method relies on two continuous signals to be sensed in the vehicle driveline; the engine torque and the vehicle speed. Information is also required about the current gear, when gearshifts occur, and when any of the braking systems present in the vehicle are activated.

Modern HDVs generally feature a distributed control system, with a number of interconnected electronic control units. These control units communicate in a network, usually an implementation of the controller area network (CAN) described in the ISO standard (11898-1:2003, 2003). The vehicles used in this study broadcast all the needed signals on their CAN buses.

The speed sensor is a part of the anti-locking brake system. This system monitors the speed of each individual wheel, to avoid lock-ups during braking. The speed is determined by counting the number of teeth on a gear passing by a pickup during a unit of time. The average of the speed sensed on the front wheels is used as the vehicle speed. The front wheels are generally not driven, except on all-wheel drive vehicles, and are as such preferable from a slip perspective.

The current gear and gearshift signals are broadcast by the gearbox control unit. If the vehicle is equipped with a manual gearbox it does not have such a unit. In that case the signals can be recreated by using the engine speed and wheel speed signals that are still present. The ratio between these speeds will either be consistent with a particular gear, in which case the conclusion is drawn that the indicated gear is engaged. If the ratio varies or is inconsistent with any gear a gearshift is signalled.

The engine torque is calculated and broadcast by the engine control unit. It is determined by the engine state, and how much fuel is injected during each cycle. The amount of injected fuel is in turn governed by how long the fuel injectors stay open. The opening times required in order to come as close as possible to

providing the torque requested by the driver are calculated by the control unit before each injection. The expected engine torque is sent on the communication bus as a percentage of the maximum torque for the engine.

2.4.2 Global Navigation Satellite Systems

Satellite based positioning systems are rapidly becoming ubiquitous not only as personal navigation devices, but also built in many complex products. In the near future it is anticipated that the majority of HDVs being sold will have at least one satellite based positioning device built in. These devices will not necessarily provide navigation services to the driver, but rather support other functions integrated into the vehicle. Various fleet management and remote surveillance services are quickly becoming essential for the operation of a modern and competitive transportation network. A basic set of such services may include periodical status updates on position, speed and fuel consumption from a vehicle to the traffic office, an alert system that triggers if a vehicle leaves its normal operating area and status updates about the vehicle condition to the function responsible for vehicle maintenance. This information stream from the vehicle enables more efficient resource utilization in fleets, increases safety, and lets the operator schedule maintenance when it is needed instead of with specific time or distance intervals.

Access to the absolute vehicle position also opens up the possibility of repeated measurement of a particular road segment using vehicle sensors. In this work we utilize this in order to update a road grade estimate each time the vehicle has passed over a certain road segment. A GPS satellite positioning device is used both as a sensor in the road grade estimator, and as the means of synchronizing data sets from multiple runs along a road.

While there are several, regional and global, satellite navigation systems available or entering service, only the GPS system has been used in this project. It is understood that any such system could be used instead, but only the term GPS will be used henceforth. Future systems will most certainly improve performance and introduce new features that can improve the performance of the proposed grade estimator.

The GPS system works by measuring the time it takes for radio signals to travel from satellites to a receiver on the ground. Knowing the speed that the radio signal propagates at, it is possible to determine the distance to each of the satellites. The positions of the satellites themselves are transmitted to the receiver at the same time as the propagation time is identified, and it is thus possible to determine the position of the receiver as well. The receiver does not in general have access to a calibrated time signal, so the current time has to be determined from the satellite signals as well. In order to determine the 3D-position of the receiver a total of four unknowns (latitude, longitude, altitude and time) have to be determined. This calculation requires four satellites to be visible. A more thorough description of the satellite navigation systems is beyond the scope of this work, but a good starting point for a general overview without too much mathematics is (El-Rabbany, 2006).

A thorough treatment of the subject, including the relevant equations, is given in (Misra and Enge, 2006).

2.4.3 GPS Positioning Errors

The accuracy of the position given by the GPS is very important for the correct functioning of the grade estimator. The error in the vertical position reported by the GPS will directly influence the estimated road grade, and the horizontal positioning error will cause grade estimates from different points on the road to merged together. Since the proposed system is designed for use in a cost-sensitive environment a standard low-cost single channel GPS receiver will have to suffice. Such a receiver delivers what is called a standard positioning service, and has a typical 10 m horizontal and 15 m vertical accuracy. The accuracy figure is given as the 95th percentile of the error distribution (Misra and Enge, 2006, page 49). The error at any given time is dependent on the receiver used as well as the atmospherical conditions, the receiver surroundings and the satellite geometry. The satellite geometry portion of the error is commonly described by a dilution of precision (DOP) number. This is broadcast by many receivers as an aid to the user in determining the quality of a given position estimate.

A particularly troublesome error source is multipath effects, that occur when both reflected and direct signals from a satellite reaches the receiver antenna. The receiver will then process the sum of all the signals, and may obtain a satellite range measurement with a large error. As the vehicle moves the reflections will change quickly. This can lead to severe noise in the delivered position. Many large reflective sources, such as mountains and buildings, are stationary and are likely to cause trouble every time the vehicle passes them.

The major error sources, except multipath, in the GPS system are slow varying, which means that measurements taken over short time intervals likely will have a bias as the major error component. Over long periods of time the GPS position estimates are bias free and the error approximately normally distributed. In our grade estimation application this means that adjacent GPS measurement points will likely have a slow varying bias, with a period of several hours. Grade estimates for a specific location however, will be based on uncorrelated normally distributed measurements. This is a prime motivation for developing a method for fusion of many measurements spread over time into one road grade estimate.

2.5 Summary

There is a growing need for accurate road grade maps due to advances in vehicle control technology. Vehicle efficiency and safety, as well as driver comfort, can be improved in a number of ways using stored road grade information. There is as of yet no standard solution to how these maps shall be obtained, even though a number of proposals for how the road grade can be estimated have already been made. Systems for estimating the instantaneous road grade have been used in

many vehicles for a while, but these cannot directly provide the preview information required by the emerging control systems.

Many different vehicle control applications that will clearly benefit from access to accurate road grade maps have been proposed in recent years. Due to the large potential for saving energy, predictive cruise control is anticipated to be an early application of preview road grade information in HDVs. In this context the presented results on the effects of road grade errors in this application are highly interesting. The analysis of road grade requirements for a predictive cruise controller in Section 2.3 indicate that 75 % of the potential gain remains with an altitude error of 1 m after a distance of 320 m. Thus the results of the proposed estimation method, with a mean bias of -0.10 % grade, and with an approximately normal error distribution around the bias with a mean standard deviation of 0.14 % grade, come forth as very promising.

An important feature of the proposed method is that only standard truck sensors are used in the road grade estimator. This opens up the possibility of mass deployment of the system, without significant hardware cost.

The current literature includes a number of proposed methods for estimating the road grade. Some are quite similar to the Kalman filter used as the first step of the grade estimator presented in this thesis. However, these methods are generally focused on estimating the instantaneous road grade only, and do not take into account the gain in accuracy that can be achieved from recording a current estimate and later having access to data from multiple runs along the road. Another class of methods aim to use data from many vehicles and/or runs, but do not include the road grade. The combination of using multiple runs and estimating the grade based on both a GPS and a vehicle model is novel.

Chapter 3

Modeling

The first step in creating the road grade estimator is to obtain a model that links the observable signals vehicle speed, v, altitude, z, and engine torque, T_e to the road grade, α. This chapter starts with a description of how a vehicle model is derived from a representation of the longitudinal dynamics of a HDV as a function of time. In order to implement the estimator we also need a model for how the road grade signal develops, this is provided in Section 3.2. Next, the two sub-models are put together into a complete description of the road-vehicle system in continuous time. To facilitate merging of measurement data from multiple runs along the road the system model is then transformed into the spatial domain and discretized. The described system model is non-linear in the vehicle speed. In order to use it in a standard Kalman filter it has to be linearized, this is described in Section 3.5. In Section 3.6 the measurement equation associated with the system model is detailed. A summary of the system model concludes the chapter.

3.1 Vehicle Model

A basic vehicle model that describes one-dimensional longitudinal movement and links engine torque, vehicle speed and road grade is sufficient to support the road grade estimation. Only the relatively low frequency dynamics of the vehicle itself are of interest. Higher frequency phenomena such as driveline oscillations and torsional vibration in the propeller and drive shafts can thus be ignored. The model is developed based on straightforward mechanical relations and Newton's laws of motion. This section provides an overview of the components included in the vehicle model, and how they are represented. More details on the various subsystems and their representation can be found in (Kiencke and Nielsen, 2003).

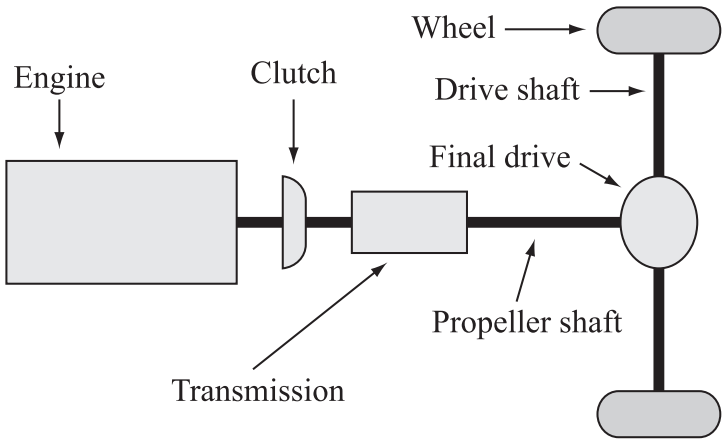

Figure 3.1: Powertrain components for a rear-driven diesel powered truck.

3.1.1 Powertrain Model

The powertrain of the vehicle includes the engine and a system to transfer power to the road surface over a broad range of vehicle velocities, while maintaining a restricted range of possible engine speeds. A Powertrain for a rear-driven vehicle consisting of engine and a driveline is shown in Figure 3.1. The various parts of the powertrain are described individually before they are put together to form a complete model. The notation for torques and angles used in the model is shown in Figure 3.2.

Engine

A typical truck engine runs on diesel fuel and has an operating range of 500–1500 rpm. Most of the internal workings of the engine are not important in our model, so it will be considered as a black box that generates torque. The one part of the engine operation that we do care about is how much torque it generates. An estimate of the generated torque is continually broadcast by the engine management system, as described in 2.4.1. The engine dynamics are the net result of torque generated from the internal combustion ($T_{\text{comb,e}}$), engine friction ($T_{\text{fric,e}}$), and the external load from the clutch (T_{c}). From Newton's second law of motion the model becomes

$$J_{\text{e}}\ddot{\alpha}_{\text{cs}} = T_{\text{e}} - T_{\text{c}} \tag{3.1}$$

where J_{e} is the mass moment of inertia of the engine including the flywheel. α_{cs} is the crankshaft angle and $\ddot{\alpha}_{\text{cs}}$ is the crankshaft acceleration. The quantity

$$T_{\text{e}} = T_{\text{comb,e}} - T_{\text{fric,e}} \tag{3.2}$$

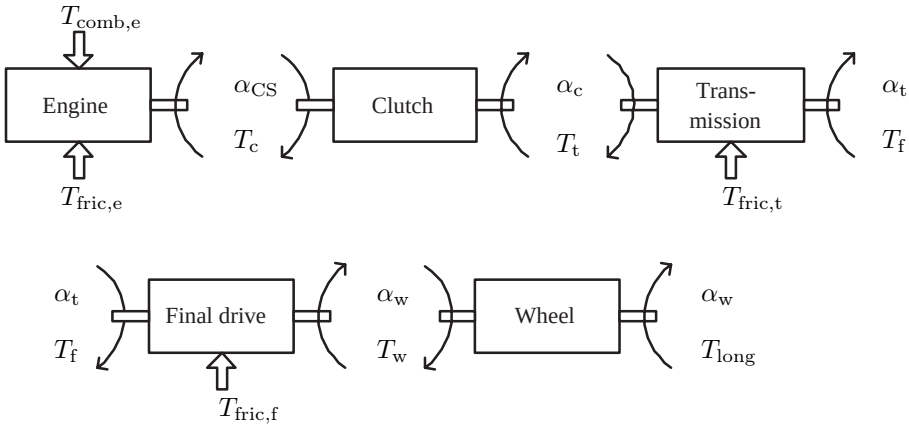

Figure 3.2: Subsystems and notation for the torques and angles used in the powertrain model.

is available as a measurement reported on the vehicle CAN bus, and will be used as an input signal in the model.

Clutch

A vehicle equipped with a manual gearbox generally has a friction clutch, that is used to disengage the engine from the rest of the driveline while idling without moving to neutral and when changing gears. In the current model idling with the clutch depressed is not distinguished from running in neutral gear, and gearshifts are considered to be instantaneous. The clutch can thus be considered as a solid massless shaft.

$$T_{\text{c}} = T_{\text{t}}, \quad \dot{\alpha}_{\text{cs}} = \dot{\alpha}_{\text{c}} \tag{3.3}$$

Transmission and Final Drive

The task of the transmission and the final drive is to match the engine speed to the wheel speed. The gear ratio in the transmission can be varied by shifting gears, while the ratio in the final drive is fixed for a particular vehicle. In each engagement of gears there is a small transmission loss incurred as power is transferred. For our purposes the loss can be modeled as a percentage of the output torque. The transmission and final drive are considered stiff, and their respective inertias are neglected. For the transmission we get

$$T_{\text{fric,t}} = (1 - \eta_{\text{t}}) i_{\text{t}} T_{\text{t}} \tag{3.4}$$

as an expression for the friction loss torque, where i_t is the current transmission gear ratio and η_t is the torque transfer efficiency for the current gear. Using this loss model the transmission model can be written as

$$\dot{\alpha}_c = \dot{\alpha}_t i_t \tag{3.5}$$

$$T_t i_t - T_{fric,t} = \eta_t T_t i_t = T_f \tag{3.6}$$

It is important to consider the angular velocity of the transmission rather than the angle, otherwise there will be an error when switching gears (changing i_t) when $\alpha_t \neq 0$).

Between the transmission and the final drive there is a propeller shaft that is not modeled (see Section 3.1.1). The final drive is described in the same way as the transmission, but the gear ratio will never change. The friction losses in the final drive are labeled $T_{fric,f}$ and calculated from the efficiency η_f. The final drive model becomes

$$\dot{\alpha}_t = \dot{\alpha}_w i_f \tag{3.7}$$

$$T_f i_f - T_{fric,f} = \eta_f T_f i_f = T_w \tag{3.8}$$

where α_w is the wheel rotation angle and T_w is the wheel torque.

The transmission ratio used in the simulation model is chosen based on the active gear. Neutral gear and open clutch situations require special care, since there is no fixed ratio between the input and output speeds in the transmission during these times. When the model is used in this work, gear shifts without clutch depression are considered to be instantaneous switches between transmission ratios. Manual gear shifts with the clutch depressed are treated as a move from the original gear into neutral, and then from neutral into the new gear. The neutral gear is represented by a zero torque transfer between the engine and the rest of the driveline.

Wheels

The driven wheels constitute the contact point where power can be transferred between the powertrain and the road. Rotation and torque in the powertrain are linked to longitudinal movement and forces acting on the vehicle through the wheels. A vehicle model including the effects of both torques and forces acting in the direction of travel can be created by transforming the powertrain torque into a longitudinal force. Under the assumption of a rolling condition (no slippage in the contact point between the tires and the ground)

$$\dot{\alpha}_w = \frac{v}{r_w} \tag{3.9}$$

and the transformation is straightforward. Here r_w is the effective wheel radius, $\dot{\alpha}_w$ is the wheel speed and v is the vehicle speed

When the vehicle speed changes the moment of inertia of all the wheels has to be overcome. For a passenger car the number of wheels is generally four. For HDVs

it can vary between six and twenty, or even more. The rotational dynamics of all the wheels are given by

$$J_{\mathrm{w}}\ddot{\alpha}_{\mathrm{w}} = T_{\mathrm{w}} - T_{\mathrm{long}} \tag{3.10}$$

where J_{w} is the total wheel moment of inertia, and T_{long} is the torque induced by the resisting forces and longitudinal mass inertia of the vehicle.

The longitudinal force from the powertrain is related to the torque through

$$F_{\mathrm{powertrain}} = \frac{T_{\mathrm{long}}}{r_{\mathrm{w}}} \tag{3.11}$$

Flexibilities and Backlash

The forces affecting a HDV driveline are large, and quite capable of twisting the driveshafts and the propeller shaft considerably. It is in fact quite possible to break the drive shafts by accelerating hard in a low gear with a heavy load. Consequently, an accurate representation of the driveline dynamics would require flexible components rather than stiff. This would allow for the representation of the energy stored in twisted shafts. The driveline flexibilities are however mainly of importance during quick changes in the transferred torque, and give rise primarily to high frequency oscillations. The road grade generally changes much more slowly, as seen in Section 3.2, and we are thus content with excluding these factors.

Play between different parts of the driveline can give rise to backlash effects when the torque changes rapidly. This also causes high frequency oscillations in the driveline. Backlash oscillations are ignored, on the same grounds as the torsional effects of the shafts.

3.1.2 External Forces Acting on the Vehicle

In addition to the influence of the powertrain, the external environment affects the vehicle in a number of ways. Air drag generates a resisting force, and so does wheel roll friction. The road topology can give rise to either a resisting or assisting force. If the brakes are applied this is regarded as a longitudinal resisting force, even though it might just as well have been included with the powertrain torques and considered as a resisting torque on the wheels.

The most important forces affecting the vehicle and the sign conventions used are shown in Figure 3.3. The forces are generally time varying, time has been left out of the equations for clarity of notation. $F_{\mathrm{powertrain}}$ has been described above.

At highway speeds the air drag can be quite considerable. For the 39 t tractor and semitrailer combination used in the experiments the air drag accounts for 41% of the total modeled resistive force when traveling at 80 km/h on a flat road. The force

$$F_{\mathrm{airdrag}} = \frac{1}{2} c_{\mathrm{d}} A_{\mathrm{a}} \rho_{\mathrm{a}} v^2 \tag{3.12}$$

is calculated based on the measured vehicle speed v, the vehicle model parameters air drag coefficient c_{d}, vehicle frontal area A_{a}, and the air density ρ_{air}. The true

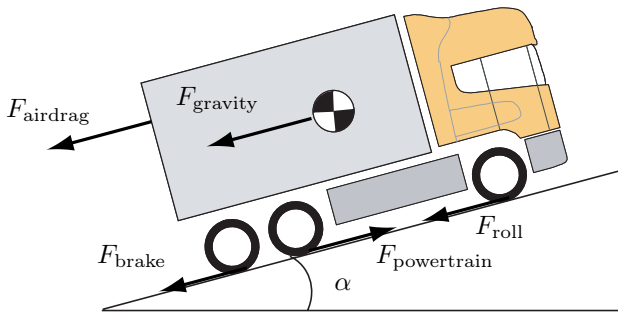

Figure 3.3: Longitudinal forces acting on the vehicle.

air density varies with meteorological conditions and the altitude. In this work the air density is described by a constant, whose value chosen to be representative for the test site temperature and altitude ranges.

A first order model gives the rolling resistance

$$F_{\text{roll}} = mgc_{\text{r}} \tag{3.13}$$

from the vehicle mass m, gravity g, and coefficient of rolling resistance c_{r}. Being proportional to the vehicle weight the rolling resistance becomes large for a fully loaded vehicle. For a very heavy, or streamlined, vehicle it will exceed the air drag. For the example vehicle above the rolling resistance accounts for the remaining 59% of the resistive force when traveling at a constant speed of 80 km/h on a flat road.

The road grade α enters the model through the gravity induced force

$$F_{\text{gravity}} = mg\sin\alpha \tag{3.14}$$

Even a small road grade generates a considerable force, for our example tractor and trailer combination, an 1% uphill grade increases the total resistive force by 84%, if the speed is unchanged.

The brake force F_{brake} is excluded from the model since it is generally unknown in a standard HDV, its effects are considered at a later stage, as described in Section 4.4.

3.1.3 Vehicle Motion

The measured quantities related to the longitudinal vehicle motion are the engine torque and the vehicle speed. The powertrain equations and the resisting forces are combined in the model in such a way that the change in vehicle speed $\dot{v}$ is expressed as a function of the current vehicle speed v, the net engine torque T_{e}, and the vehicle parameters. In order to determine this function the rotational moments of inertia in

the powertrain are combined with the longitudinal mass inertia into a total inertial mass through the gear ratios and efficiencies already described

$$m_{\mathrm{t}} = m + \frac{J_{\mathrm{w}}}{r_{\mathrm{w}}^2} + \frac{i_{\mathrm{t}}^2 i_{\mathrm{f}}^2 \eta_{\mathrm{t}} \eta_{\mathrm{f}} J_{\mathrm{e}}}{r_{\mathrm{w}}^2} \tag{3.15}$$

Since we have now accounted for the powertrain inertias through the total mass the powertrain longitudinal force becomes

$$F_{\mathrm{powertrain}} = \frac{i_{\mathrm{t}} i_{\mathrm{f}} \eta_{\mathrm{t}} \eta_{\mathrm{f}}}{r_{\mathrm{w}}} T_{\mathrm{e}} \tag{3.16}$$

Through Newton's second law of motion we get

$$\dot{v}(t) = \frac{1}{m_{\mathrm{t}}} (F_{\mathrm{powertrain}} - F_{\mathrm{airdrag}} - F_{\mathrm{roll}} - F_{\mathrm{gravity}}) \tag{3.17}$$

as a model for the vehicle velocity.

3.2 Road Model

In order to estimate the road grade using a Kalman filter we need a model for how it changes over time. Roads are built according to specifications determined by construction engineers. For every type of road and legislative region there are regulations that transcribes into requirements for the design. An efficient way of determining the road grade could be to request it from the authority who approved the design. With knowledge of the quality requirements for the constructions process, and the planned road layout it should, in theory, be possible to get a road grade estimate within a known error interval. Unfortunately reality does not agree with theory in this case and construction data is rarely readily available. Some benefits can nevertheless be had from studying road building specifications, since they give a basic idea of what type of dynamics might be expected in the road grade signal.

The specifications for Swedish roads give a good starting point for a model to describe highway road grades. The Swedish road authority has published a document, "Vägars och gators utformning" (Swedish Road Authorities, 2004), that lists requirements and guidelines for all current road construction. Some existing roads may not fully comply with these guidelines, but they will nevertheless serve as a starting point for our road model. The road grade estimation method described in this work is focused on estimating highway grades. As seen in Table 3.1 the requirements state that a highway should preferably have a road grade below 6%. The grade may only exceed 8% during short periods and due to exceptional circumstances (Swedish Road Authorities, 2004, p 102). The desired road quality has to be chosen at design time, and is related to the expected traffic load. These numbers may be higher for highways in other countries, as the topography of for

Table 3.1: Maximum allowable road grade for various road quality classes in Sweden. Excerpt of table 13 – 1 in (Swedish Road Authorities, 2004)

	High Standard	Medium Standard	Low Standard
Countryside	6%	7%	8%
Urban, main road	6%	7%	8%
Urban, intersection	2.5%	3.5%	9%

example the Alps would most certainly be regarded as exceptional circumstances by Swedish standards.

Furthermore, the document states that vertical road profile should be made up from segments with constant grade and vertical curves. The concave curves, going into more uphill gradients, are described by the parabola given by

$$\Delta z = \frac{d^2}{2R} \tag{3.18}$$

where Δz is the relative altitude, d is a horizontal distance measure relative to the lowest point of the parabola, and R is a design parameter. For the magnitudes of d used in this application the parameter R essentially represents the radius of a circular arc similar to the specified parabola. The part of the parabola to use is determined by the road grades at the start and end of the vertical curve. For convex vertical curves, i.e. hilltops, the parabola is flipped upside down.

The designed size of the parabolas depend on a number of factors:

- Traffic safety
- Driving dynamics
- Visibility conditions
- Terrain
- Esthetics

The chosen vertical arc length and radius parameter have to match the surrounding terrain, and provide sufficient visibility for drivers to be able to stop before unexpected obstacles. This is particularly an issue for convex vertical curves, i.e. hilltops. For a major highway to be considered to have a good visibility standard when designed for a velocity of 110 km/h the minimum convex vertical curve radius, as listed in Table 3.2, is $R = 16000$ m. If the arc length is so short that it does not limit visibility the limiting requirement becomes comfort, and the limit

Table 3.2: Minimum convex vertical curve radius for roads with at least two lanes with regard to sight distance for passenger cars. High, medium, and low refers to the chosen visibility standard for the road. Excerpt of table 11 − 1 in (Swedish Road Authorities, 2004)

V_{ref}	Environment	High	Medium	Low
50	Urban, main road	1200	400	300
70	Countryside	3000	1800	1200
70	Countryside	3000	1200	1800
90	Countryside	7000	6000	5000
110	Countryside	16000	13000	9000

is $R = 2200$ m. There are also regulations in place requiring a certain density of overtaking opportunities. In order to provide enough sight distance for overtaking on a convex vertical curve, a radius on the order of $R = 100000$ m is required.

For concave vertical curves the constraint on minimum radius for arc lengths long enough to limit visibility is $R = 6500$ m on major highway with a high visibility standard. If the maximum speed is restricted to 90 km/h it is allowed to design with $R = 4500$ m for high visibility standard, and $R = 3500$ m for low visibility standard. These limitations are based on requirements for headlamps and their illumination cone. A potential obstacle in a vertical curve must be illuminated in time for the driver to have a chance to stop before impact. For short arc lengths, which do not limit visibility, the limits are the same as for convex curves.

Based on the assumption that the vertical road profile can only consist of segments with constant road grade, or parabolic segments as described above we obtain two different road models with the distance along the road as the independent variable

$$\dot{\alpha}(s) = \pm\frac{1}{R} \tag{3.19}$$

where the road grade is changing, and

$$\dot{\alpha}(s) = 0 \tag{3.20}$$

on constant grade segments.

Since the true road model, assuming the road has been built as prescribed by today's standard, varies with distance the task of choosing a suitable representation becomes a delicate one. Given that the minimum R on a major highway, for any sizeable change in the road grade, is $R = 3500$ m the maximum magnitude of the change in the road grade given a percentage points per meter traveled is

$$\max\dot{\alpha}(s) = \frac{1}{3500} \approx 0.029 \tag{3.21}$$

Using the road grade model that only allows for a constant rate of change in the grade based on a parameter discretely changing R introduces the added difficulty of estimating that parameter in addition to the grade itself. Since R changes discretely this would lead to a hybrid continuous/discrete estimation problem. On the other hand, if the process variance for the road grade state is chosen large enough, we can disregard the low frequency bias introduced by the road designer. Thus we adopt a road grade model that is sometimes right, and at other times represents the middle ground between convex and concave vertical curves. The model

$$\dot{\alpha}(s) = 0 \tag{3.22}$$

is adopted for all situations.

The road grade is the derivative of the altitude, so the road altitude model becomes

$$\dot{z}(s) = \sin\alpha(s) \tag{3.23}$$

in spatial coordinates and

$$\dot{z}(t) = v(t)\sin\alpha(t) \tag{3.24}$$

when expressed indexed in time.

3.3 System Model

Based on the described models for the vehicle on the road, and the road itself we can put together a model for the complete system. We define a state vector

$$x(t) = \begin{bmatrix} v(t) \\ z(t) \\ \alpha(t) \end{bmatrix} \tag{3.25}$$

containing the vehicle velocity, the road altitude and the road slope. Using

$$m_{\mathrm{t}} = \frac{J_{\mathrm{w}} + m r_{\mathrm{w}}^2 + i_{\mathrm{t}}^2 i_{\mathrm{f}}^2 \eta_{\mathrm{t}} \eta_{\mathrm{f}} J_{\mathrm{e}}}{r_{\mathrm{w}}^2} \tag{3.26}$$

and the expressions presented earlier for the magnitudes of the forces involved we can define the system model

$$\underbrace{\begin{bmatrix} \dot{v}(t) \\ \dot{z}(t) \\ \dot{\alpha}(t) \end{bmatrix}}_{\dot{x}(t)} = \underbrace{\begin{bmatrix} \frac{i_{\mathrm{t}} i_{\mathrm{f}} \eta_{\mathrm{t}} \eta_{\mathrm{f}}}{r_{\mathrm{w}} m_{\mathrm{t}}} T_{\mathrm{e}}(t) - \frac{\frac{1}{2} c_{\mathrm{d}} A_{\mathrm{a}} \rho_{\mathrm{a}}}{m_{\mathrm{t}}} v(t)^2 - \frac{mg}{m_{\mathrm{t}}}(c_{\mathrm{r}} + \sin\alpha(t)) \\ v(t)\sin\alpha(t) \\ 0 \end{bmatrix}}_{f(v,\alpha,T_{\mathrm{e}})} \tag{3.27}$$

where the time dependence of the states and the input net engine torque signal has been made explicit. Then engine torque is measured and regarded as a known

input signal in the model, $u(t) = T_{\mathrm{e}}(t)$. Since the transmission ratio and associated efficiency are dependent on the engaged gear the model changes discretely at gear changes. Additionally, since the driveline friction always causes an energy loss in the direction energy is flowing, the efficiencies η_{t} and η_{f} depend on whether the net engine torque T_{e} is positive or negative. Whenever the power flow from the engine to the wheels is negative, the efficiencies become the inverse of their nominal values, causing another discrete switch in the system model.

3.4 Spatially Sampled System Model

In order to easily obtain estimates at specific spatial locations rather than time instants a spatially sampled version of the model is derived. This is a prerequisite in order to effortlessly merge road grade estimates from multiple runs along a road.

After the change of independent variable the model is discretized using the step length Δs. By resampling measurement data from different runs along the road to represent common spatial coordinates a consistent merge can be performed. The purpose of our model is to serve in a Kalman filter to estimate the states, so we also need to add process noise to account for disturbances. One white noise process is added to each of the model states. The discretized model becomes

$$\underbrace{\begin{bmatrix} v_k \\ z_k \\ \alpha_k \end{bmatrix}}_{x_k} = \underbrace{\begin{bmatrix} v_{k-1} + \Delta s \frac{dv_{k-1}}{ds} \\ z_{k-1} + \Delta s \sin \alpha_{k-1} \\ \alpha_{k-1} \end{bmatrix}}_{f_k(x_{k-1}, u_k)} + \underbrace{\begin{bmatrix} w_k^v \\ w_k^h \\ w_k^\alpha \end{bmatrix}}_{w_k} \tag{3.28}$$

The rate of change in velocity is given by

$$\frac{dv_{k-1}}{ds} = \frac{i_{\mathrm{t}} i_{\mathrm{f}} \eta_{\mathrm{t}} \eta_{\mathrm{f}}}{r_{\mathrm{w}} m_{\mathrm{t}}} \frac{T_{\mathrm{e}k-1}}{v_{k-1}} - \frac{\frac{1}{2} c_{\mathrm{d}} A_{\mathrm{a}} \rho_{\mathrm{a}}}{m_{\mathrm{t}}} v_{k-1} - \frac{mg}{m_{\mathrm{t}}} \frac{1}{v_{k-1}} \left(c_{\mathrm{r}} + \sin \alpha_{k-1} \right) \tag{3.29}$$

Again, the model parameters depend on the selected gear and the direction of power flow in the driveline, making this a time-varying discrete model with traveled distance along the road as the independent variable.

3.5 Linearized System Model

To evaluate the influence of the nonlinearity in the vehicle model a piecewise constant linear version of the model is also derived. The linear model is changed at gear changes and when the direction of power flow in the driveline changes. Each gear and power flow direction will lead to a different mode, denoted by an index m added to the relevant variables. For each mode a specific torque is required to maintain a constant speed, and equilibrium in the model. The linearization point thus changes as well when the model parameters change. The linear discretized

model around the equilibrium x_m is given by the system transition matrix F_m and the input matrix G according to

$$\tilde{x}_k = F_m \tilde{x}_{k-1} + G\tilde{u}_k + w_k \tag{3.30}$$

where $\tilde{x} = x - x_m$ is the state relative to the linearization point and $\tilde{u} = T_\mathrm{e} - T_{\mathrm{e}m}$ is the engine torque difference from the equilibrium torque. The transition matrix is given by $F_m = I + \frac{\partial f}{\partial x}\Big|_{x_m, u_m} \Delta s$. Using the model from before F_m and G become

$$F_m = \begin{bmatrix} 1 + \frac{dv_m}{ds}\Delta s & 0 & -\frac{mg}{m_{\mathrm{t}m} v_m}\cos\alpha_m \Delta s \\ 0 & 1 & \cos\alpha_m \Delta s \\ 0 & 0 & 1 \end{bmatrix} \tag{3.31}$$

$$G = \begin{bmatrix} \frac{i_{\mathrm{t}m} i_\mathrm{f} \eta_{\mathrm{t}m} \eta_{\mathrm{f}m}}{r_\mathrm{w} m_{\mathrm{t}m} v_m} \Delta s \\ 0 \\ 0 \end{bmatrix} \tag{3.32}$$

where

$$\frac{dv_m}{ds} = -\frac{i_{\mathrm{t}m} i_\mathrm{f} \eta_{\mathrm{t}m} \eta_{\mathrm{f}m}}{r_\mathrm{w} m_{\mathrm{t}m}} \frac{T_{\mathrm{e}m}}{v_m^2} - \frac{\frac{1}{2} c_\mathrm{d} A_\mathrm{a} \rho_\mathrm{a}}{m_{\mathrm{t}m}} + \frac{mg}{m_{\mathrm{t}m} v_m^2}(c_r + \sin\alpha_m) \tag{3.33}$$

The equilibrium point x_m for the most common mode, cruising under engine power on the top gear, is obtained by choosing $v_m = 80$ km/h, $z_m = 0$ m, $\alpha_m = 0\%$ grade, and the nominal vehicle specific values for i_{tm}, η_{tm}, and η_{f_m}. The driveline efficiencies and transmission gear ratio will also directly give $m_{\mathrm{t}m}$. As a result we get the input torque equilibrium

$$T_{\mathrm{e}m} = \frac{\frac{1}{2} c_\mathrm{d} A_\mathrm{a} \rho_\mathrm{a} v_m^2 + r_\mathrm{w} mg(c_\mathrm{r} + \sin\alpha_m)}{i_{\mathrm{t}m} i_\mathrm{f} r_\mathrm{w} \eta_{\mathrm{t}m} \eta_{\mathrm{f}m}} \tag{3.34}$$

for each mode of the linear system.

3.6 Measurement Equation

Two measured states and the input signal engine torque, T_e, are available for estimation of the system model state. The measured states are the vehicle velocity v and the altitude z. This leads to a linear measurement equation

$$y_k = \underbrace{\begin{bmatrix} 1 & 0 & 0 \\ 0 & 1 & 0 \end{bmatrix}}_{H_k} \underbrace{\begin{bmatrix} v_k \\ z_k \\ \alpha_k \end{bmatrix}}_{x_k} + \underbrace{\begin{bmatrix} e_k^\mathrm{v} \\ e_k^\mathrm{z} \end{bmatrix}}_{e_k} \tag{3.35}$$

that is used with both the linear and non-linear vehicle models. The measurement noise for the two states is described by the white noise processes e_k^v and e_k^z respectively.

3.7 Summary

A discrete spatially sampled nonlinear model for the combined system made up of a HDV on a road has been derived as (3.28). The vehicle model is based on the longitudinal motion of a vehicle with a stiff driveline as obtained from Newton's laws of motion. The road grade is modeled as a random walk, since the magnitude of deterministic change in the road grade over one distance step is very small, even for the sharpest vertical bends allowed on a highway. The road altitude is described as a primitive function for the road grade. A linearized version of the system model is also derived, and given as (3.30), it is later used to asses the effect of the nonlinearity in the original model for the data collected in the field test.

Chapter 4

Iterative Road Grade Estimation

Based on the model created in the previous chapter Kalman filtering is used to get state estimates from measured data. Two different filters are investigated; an extended Kalman filter that uses the non-linear vehicle model, and a standard Kalman filter that is based on the linearized version of the vehicle model. Section 4.1 outlines the different steps of the road grade estimation. In Section 4.2 the Kalman filter used for state estimation and smoothing is described. This is followed by a discussion on fusion of estimation results from multiple measurements in Section 4.3. The selection of appropriate noise covariance matrices Q and R is treated in Section 4.4. This is followed by a chapter summary that also includes a discussion on the chosen filtering approach.

4.1 State Estimation

Figure 4.1 shows a schematic view of how the available sensor signals are used together with previously stored road grade information to generate an updated map. Three signals, the vehicle velocity v, the absolute altitude from the GPS z, and the engine torque T_{e} are used directly with the model and Kalman filters to produce road grade estimates. The selected gear signal is used to choose appropriate values for the time-varying parameters in the system model. The Kalman filters also need the error covariance matrices Q and R to be set. These are adjusted based on the number of available satellites, if the vehicle is shifting gears, or whether the brakes are applied. The exact choice of Q and R in each situation is detailed in Section 4.4.

Once a the Kalman filter has produced a complete system state trajectory estimate for a segment of the road, this segment is processed again by a smoothing step, in order to use all recorded sensor information for the estimation at each distance index. The smoothed grade and altitude estimates are then fused with any existing data for the road segment. Finally, the new road grade map segment is stored to the database.

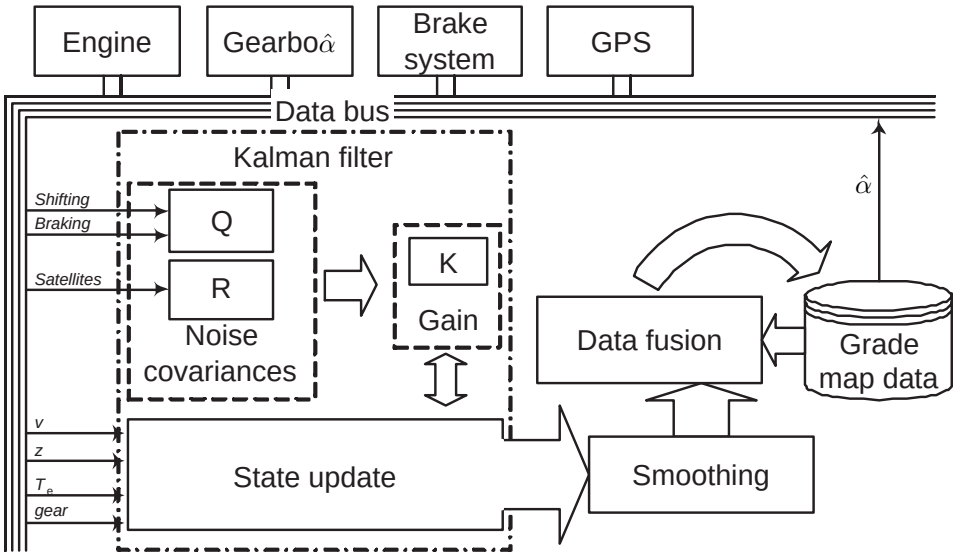

Figure 4.1: Overview of the data filtering, smoothing and fusion of the proposed road grade estimation method.

4.2 Kalman Filtering

Two different Kalman filters are used to estimate the road grade and other model states. The non-linear vehicle model is used together with an EKF, and the piece-wise linear model with a standard Kalman filter (KF). Using the notation of the previous chapter, the vehicle model to be used in the filtering with the EKF is given by

$$\begin{aligned} x_k &= f(x_{k-1}, u_k) + w_k \\ y_k &= Hx_k + e_k \end{aligned} \tag{4.1}$$

Only the state update is non-linear, the output model simply indicates that two of the states are directly measurable.

In the EKF the non-linear model is linearized around the current state at every time step. The obtained transition matrix F_k is then used to complete the steps of the standard Kalman filter recursions. These recursions are described by two update steps: a time update, or prediction, step and a measurement update. In the time update the system model is used to predict the future state of the system. Using the notation $\hat{x}_{k|k-1}$ to denote the quantity $\hat{x}$ at time k based on information

available up to time $k-1$ the time update is done according to

$$\begin{aligned} \hat{x}_{k|k-1} &= f(\hat{x}_{k-1|k-1}, u_k) \\ P_{k|k-1} &= F_k P_{k-1|k-1} F_k^T + Q_k \end{aligned} \tag{4.2}$$

Similarly to F_m in the piecewise linear model the transition matrix F_k is defined to be the Jacobian $F_k = \frac{\partial f}{\partial x}(\hat{x}_{k-1|k-1}, u_k)$. $P_{k|k-1}$ is the estimated error covariance, and $Q_k = E[w_k^2]$ is the process noise covariance. After the time update the measurement at time k is used in a measurement update to improve the estimate. The measurement update is described by

$$\begin{aligned} K_k &= P_{k|k-1} H^T (H P_{k|k-1} H^T + R_k)^{-1} \\ \hat{x}_{k|k} &= \hat{x}_{k|k-1} + K_k (y_k - H\hat{x}_{k|k-1}) \\ P_{k|k} &= (I - K_k H) P_{k|k-1} \end{aligned} \tag{4.3}$$

Here K_k is the Kalman gain, and $R_k = E[e_k^2]$ is the measurement noise covariance.

The piecewise constant linear model is used with a standard Kalman filter. At each mode change between different linearizations of the model the final state of the old filter is used to initialize the new filter. The linear system model in each mode is

$$\begin{aligned} \tilde{x}_k &= F_m \tilde{x}_{k-1} + G\tilde{u}_k + w_k \\ \tilde{y}_k &= H\tilde{x}_k + e_k \end{aligned} \tag{4.4}$$

where $\tilde{y}_k = y_k - Hx_m$. This leads to the KF time update equations

$$\begin{aligned} \hat{x}_{k|k-1} &= F_m \hat{x}_{k-1|k-1} + Gu_k \\ P_{k|k-1} &= F_m P_{k-1|k-1} F_m^T + Q_k \end{aligned} \tag{4.5}$$

The measurement equations are identical to the EKF case.

4.2.1 Smoothing

By carrying out the road grade estimation off-line, when complete longer road segment has already been recorded, it is possible to use smoothing to compensate for the filtering delay and include later measurements in the estimate for each data point. The Rauch-Tung-Striebel fixed point smoothing algorithm, introduced in (Rauch *et al.*, 1965), is used to find $\hat{x}_{k|N}$ where N is the total number of data points collected during one run along the road segment. These are the best available estimates at each position based not only on the measurements up to that position, but on all estimates collected on the road segment. The smoothing is performed backwards along the road segment, and uses quantities generated by the Kalman filter.

The predicted quantities at the last position of the road segment, where $k = N$, are used to initialize the recursion. This gives access to $P_{N+1|N}$ and $\hat{x}_{N+1|N}$ in the

firs step of the smoothing recursion. P_k^s denotes the smoothed error covariance, $\hat{x}_k^s$ is the smoothed state estimate, and K_k^s is the smoothing gain. The smoothing backwards recursion is given by

$$\begin{aligned} K_k^s &= P_{k|k} F_k^T P_{k+1|k}^{-1} \\ \hat{x}_{k|N}^s &= \hat{x}_{k|k} + K_k^s(\hat{x}_{k+1|N}^s - \hat{x}_{k+1|k}) \\ P_{k|N}^s &= P_{k|k} + K_k^s(P_{k+1|N}^s - P_{k+1|k}){K_k^s}^T \end{aligned} \tag{4.6}$$

4.3 Data Fusion

In order to merge data from many runs along the same road segment a distributed data fusion method is used. The distributed approach has the important advantage that the amount of road data that has to be stored does not increase as additional estimates from known road segments are incorporated into the map. For each road segment, the map consists of the road related states (altitude z and grade α) and the associated estimated error covariance estimates for those states. The vehicle velocity is not of any interest in the map, since it is not a road property. Based on the estimated error covariances stored in the map and the estimated error covariances of a new smoothed estimate an updated map is created each time a new estimate of a road segment becomes available.

Assuming that the errors in estimates from each run along the road are entirely uncorrelated, the quantities for the new map can be calculated as follows

$$\begin{aligned} P_k^f &= ((P_k^1)^{-1} + (P_k^2)^{-1})^{-1} \\ \hat{x}_k^f &= P_k^f((P_k^1)^{-1}\hat{x}_k^1 + (P_k^2)^{-1}\hat{x}_k^2) \end{aligned} \tag{4.7}$$

where P_k^f is the resulting error covariance, $\hat{x}_k^f$ is the new state estimate for the map. The quantities P_k^1, P_k^2, $\hat{x}_k^1$, and $\hat{x}_k^2$ are the source estimates and estimated error covariances. This data fusion method is described in more detail in e.g. (Gustafsson, 2000).

The assumption in (4.7) that estimation errors in the two source samples are uncorrelated is troublesome. Since the estimates are based on repeated measurements using the same method, and of the same system realization, it is unlikely that this is fully satisfied. This discrepancy will lead to an underestimate of the state error covariances in P_k^f. Over time this will lead to new estimates having little influence on the already stored data. In practice it may very well be desirable to have the opposite behavior. Roads are occasionally modified, so it may be good practice to eventually forget very old data, i.e. weight the new estimate higher than what would be indicated by P_k^f.

Another important caveat is that in practice covariance terms between the altitude and road grade states, represented by the off-diagonal terms of the source matrices P_k^1 and P_k^2 actually degrade the merged result. Uncertainties in the estimation of these quantities in the Kalman filtering and smoothing steps occasionally

cause the weighting factors to give a combined estimate that is not in the interval $[\hat{x}_k^1, \hat{x}_k^2]$. Currently this problem is solved by only using the diagonal elements of P_k^1 and P_k^2 in the fusion. The result is that only the estimated covariance of each of the states will affect how much weight the measurement of that state has in the merge, the estimated cross correlation between altitude and road grade errors will be ignored.

When a map is first created based on estimates from two runs a long the road both the source sets are smoothed results from individual runs, after that one source will be the map (based on all previous measurements), and one will be the new estimate to be incorporated.

4.4 Selection of Q and R

One of the main challenges in using the grade estimation method on real data is that the true noise covariances Q and R are not known. In the current method they are instead used as design variables to tune the grade estimation filter to generate an accurate and reliable estimate.

To simplify the choice of these design parameters the noise covariance matrices were chosen to be diagonal. For the measurement noise this seems reasonable since the vehicle speed and GPS altitude are obtained through independent sensors measuring different quantities, whose measurement error can be assumed independent. For the process noise the situation is more complicated. Unmodeled changes in the road grade are likely to show up also in the running sum of the road grade multiplied by the sample distance, i.e. the distance. It is also likely that such an error would have an effect on the velocity error as well, since the road grade used in that calculation is faulty. The magnitudes of these effects are hard to estimate beforehand, since they depend on the magnitudes of the model errors themselves. In this first version of the method the results when using a diagonal Q matrix are investigated, evaluation of what improvements could be had with a full matrix are left as future work.

For normal driving at a fixed gear the process noise Q is tuned to be as small as possible while still allowing the road grade estimate to follow the reference road grade closely during unmodeled transitions between flat road and constant grade inclines, as discussed in Section 3.2. Driving events such as gearshifts and braking affect the vehicle in ways that are not covered by the relatively simple vehicle model given in Chapter 3. To account for this the process variance for the velocity state is increased when such events occur. During braking no useable torque estimate is generally available, so the only action taken in the filter is to reduce the reliance on velocity predictions. During gearshifts it can be assumed that the engine torque that comes through the driveline and affects the vehicle will be low. With a manual gearbox this is true since the clutch will be depressed during shifting. With an automated manual gearbox the same holds since the gearbox controller will take over engine control to achieve matching input and output transmission speeds as well

as zero torque transfer in order to switch gears without clutch engagement. Driveline oscillations as well as drive and propeller shaft torsion can cause considerable torques, but the average value of these on the time scale of interest is limited. The net engine torque during braking is assumed to be zero in the model, regardless of the value reported from the vehicle.

The measurement noise R is adjusted depending on the number of GPS satellites available. While other GPS-system related factors also affect the GPS position accuracy, the number of satellites is the only relevant signal that is available from the satellite receiver used. When satellite coverage was lost, a very high variance for was set for the altitude measurement. This causes the grade estimate only to depend on vehicle signals. Even during ideal conditions the noise in the GPS altitude signal can be considerable, so the error covariance was to be chosen relatively high all the time. An issue worthy of future attention is whether it would be worthwhile to improve the GPS sensor model to include more than just the true value and additive white noise. It should be noted that the chosen noise covariance during nominal conditions for the GPS altitude measurement is large enough to essentially saturate the influence through the filter equations that it can have on the estimated grade error covariance $P(3,3)_k$. Thus, the estimated error covariance for the grade state does not currently increase noticeably when satellite loss occurs.

4.5 Summary

A road grade estimator based on standard HDV sensors has been developed on the form shown in Figure 4.1. The estimator uses a Kalman filter where the noise and process variances are adapted to driving events. Estimation is carried out after a run along one road segment has been completed and smoothing can thus be used to improve accuracy and avoid time-lag issues. The estimator produces spatially sampled estimates, that are fused together with the aggregate of previous estimates of the road grade at that location. As shown in Figure 4.2 the fused final result of the estimate based on six experiments agrees well with a reference grade profile for the road segment.

The Kalman filter in the estimator is known to produce an optimal state estimate in the minimum mean square error sense, given that the system is linear and that the measurement and process noises are truly white, Gaussian, and have the assumed covariances. Since we have a non-linear system, with model and sensor errors that most likely yield somewhat colored process and sensor noises, there is no proof neither that the estimates will be optimal, nor that they will even converge. The RTS smoothing similarly provides minimum mean square error estimates of the state at each position based on all the collected measurements, for systems that fulfill the same assumptions as for the Kalman filter. As we are using our EKF results as input to the smoothing recursion there is no proof that the output will be optimal, or that it will converge. Using the linearized model only moves the non-compliance with assumptions about the model to the assumptions about the noises.

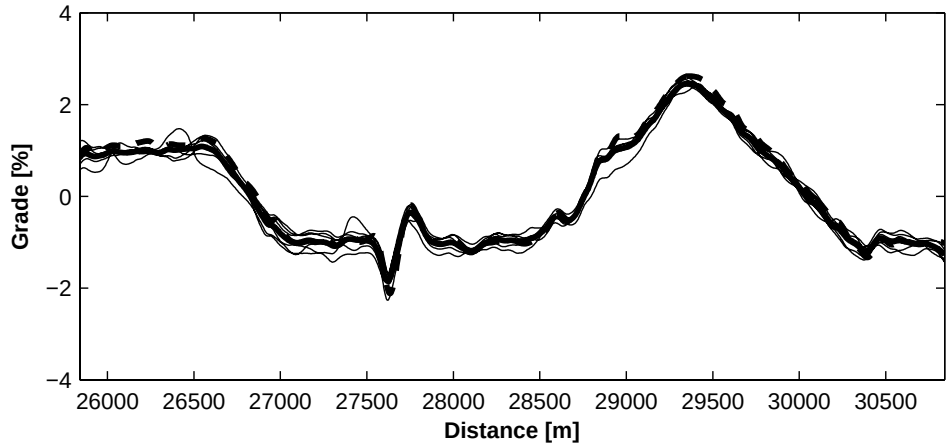

Figure 4.2: The final grade estimate, for a segment in the southbound experiments, calculated using the proposed grade estimator based on six experiments is shown (solid) together with the reference grade profile from a specialized measurement vehicle (dashed). The estimates from the individual experiments are also included (thin lines).

In this case not only the previously existing model errors, but also linearization errors contribute to coloring the noise.

Similarly, optimal estimation based on all available experiments would yield a very large Kalman filter, including two states to describe the road, and one velocity state for the vehicle used in each experiment. By only fusing the road states based on their estimated error covariances, the problem of including models for all the vehicles in the filter is avoided. As a consequence the estimate will no longer be optimal. The applied fusion method includes the assumption that the different experiments observe the system with different realizations of the process noise. In our case this is not true, the road realization is the same each time the vehicle passes over it. When the process noise is correlated between experiments, the distributed fusion will underestimate the error covariance matrix. As noted in Section 4.3 issues with the estimated cross-correlation between the altitude and slope states further moves the implemented method away from the theoretical optimum.

Chapter 5

Experiments

The proposed road grade estimation algorithm has been tested on experimental data collected using HDVs driving on a Swedish highway. The road tests verify the applicability of the method, but also provide insights on areas of possible future improvements. This chapter describes the experiments that have been made and the obtained results. The first two sections describe the road tests in general and the test vehicles. The next section relates the experiments to the grade estimator as it is described in Chapter 4. This is followed by an account of the data post-processing steps required for completion of the road grade estimation. Next, the experimental results are given in a comprehensive breakdown of the performance of the road grade estimator under the various conditions faced during the tests. The final section of the chapter summarizes the experimental results.

5.1 Road Tests

Road tests with the proposed grade estimation algorithm have been carried out on a part of highway E4 from Södertälje to Nyköping, as shown in Figure 5.1. The test road contains a mix of hills with road grades between $-4\,\%$ and $4\,\%$ and flat segments. This gives an opportunity to study how the estimation algorithm handles various situations such as hill climbing using maximum engine torque, hill descent with no brakes applied, hill descent while using the brakes, and steady state driving on relatively flat road.

To illustrate details in the behavior of the road grade estimation algorithm results are presented for the full 29 km long southbound, and 38 km long northbound road segments, as well as short segments that represent the driving scenarios detailed above. In order to effectively evaluate the obtained road grade estimates a reference grade profile is required. The reference profile used in this work has been obtained from a high quality 3D trajectory measurement system based on a tightly coupled GPS and inertial navigation system, as described in Section 5.5.

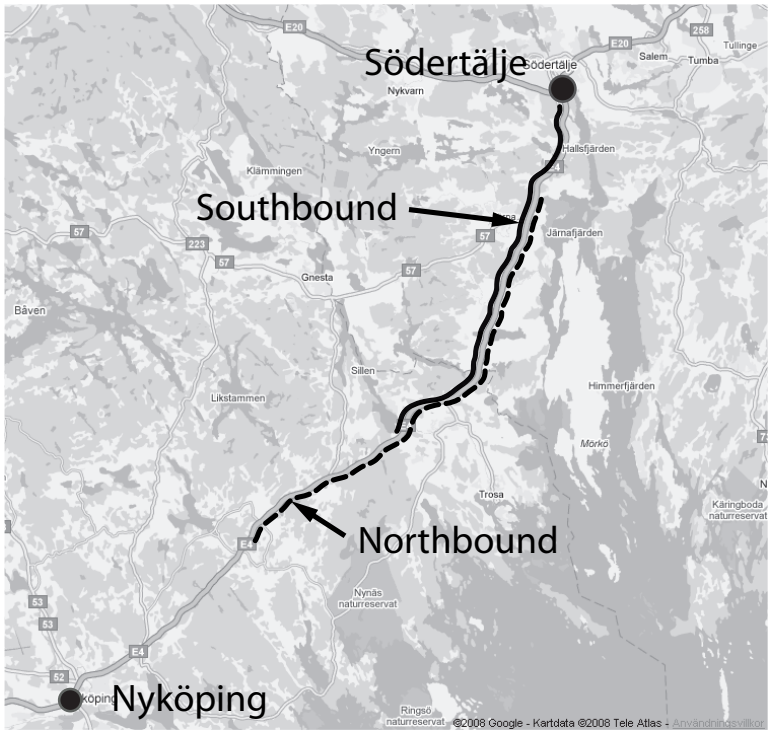

Figure 5.1: Map of the test area. Experiments have been conducted on highway E4 between Södertälje and Nyköping. (Image courtesy of Google)

5.2 Test Vehicles

The configuration and important parameters of a HDV can vary substantially, therefore three different vehicles have been used to verify the applicability of the grade estimation method in each case. The types of test vehicles used are illustrated in Figure 5.2. The weight of a HDV in Sweden typically varies between 8 t for a small empty truck and 60 t for a fully loaded large vehicle combination. On most European markets the maximum allowable weight is 40 t. The test vehicles have weights ranging from 12 t to 39 t and between 2 and 5 axles. Important properties for the test vehicles are listed in Table 5.1.

The modeled external forces described in Section 3.1.2 depend heavily on the vehicle parameters used in the equations. Getting reasonable values for these can be a challenge, especially when they are supposed to describe a vehicle in day to day operations rather than in a laboratory setting. In this work the vehicle parameters have been chosen as representative values for the vehicle types that have been used.

Figure 5.2: Test vehicles used for road tests of the grade estimation algorithm. Three vehicle configurations were used. Starting from the left they were a tractor-semitrailer combination (A), tractor only (B), and rigid truck (C). (Photographs courtesy of Scania CV AB)

Table 5.1: Key properties and specifications for the test vehicles used to collect experimental data. The total vehicle weight is given in tons.

Vehicle	Type	Configuration	Weight	Axles	Meas.
A	P310LA4x2MNA	Tractor and semi-trailer	39 t	5	1,2,3
B	R420LA4x2MNA	Tractor	12 t	2	4,5
C	R420LB6x2*4MNB	Rigid truck	21 t	3	6

A total of six round-trip experiments have been conducted on the test road. The total vehicle weight in each experiment is assumed to be known in the road grade estimator, so it has been measured using a scale. The different vehicles were driven on different days and under varying weather conditions, but a nominal air density figure was still used for all experiments. The experiments with vehicle A were conducted during testing of a look-ahead vehicle speed controller. This represents a very likely scenario for a recursive road grade estimation application, since a truck equipped with a look ahead speed controller with a self-learning map engine can be assumed to operate with the controller enabled. There are currently not enough directly comparable measurements to conclude if estimation while operating with this speed controller yields results that significantly differ from for example a constant speed controller. However, the overall accuracy of the estimation results when using the look ahead speed controller is likely be somewhat higher due to the reduction in braking and gear-shifting.

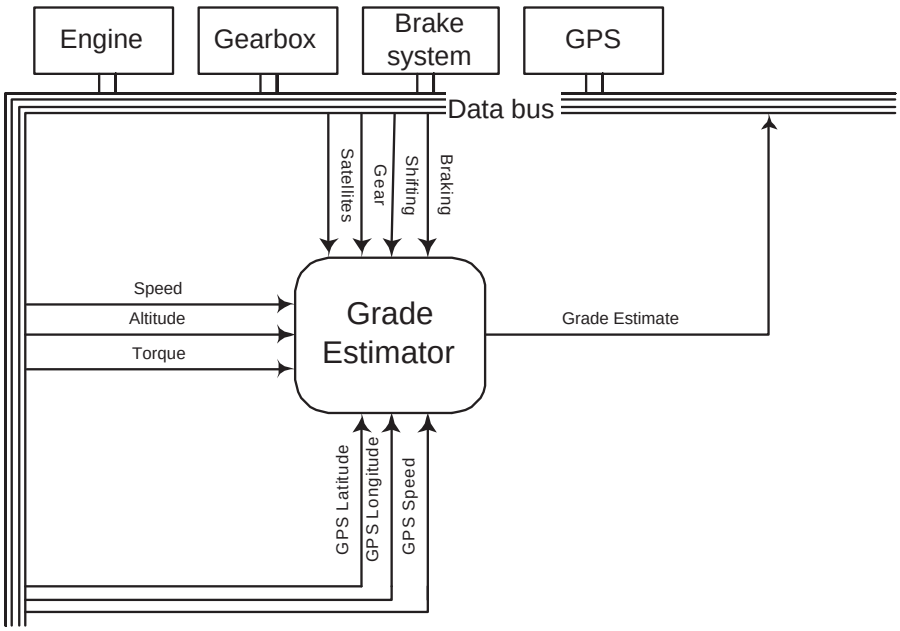

Figure 5.3: The grade estimator described in Chapter 4 and illustrated in Figure 4.1 depends on two directly measured states, the speed and the altitude and the engine torque which is treated as a measured input signal. The estimator also relies on auxiliary information about when braking and gearshifts occur, the currently engaged gear and the number of tracked GPS satellites. Finally, additional GPS signals are recorded to enable fusion of road grade estimates from multiple runs along a road.

5.3 Experimental Setup

The proposed road grade estimation algorithm depends on measurements of a number of vehicle state variables, as shown in Figure 5.3. The vehicle speed, v, the current altitude, z and the instantaneous engine torque, T_e, shown on the left side in Figure 5.3, are all used directly in the road grade estimation. They are treated further in Sectino 5.3.1. In addition to these a number of signals are needed for proper adaptation of the grade estimator to changes in the vehicle and the environment, these are shown entering the grade estimator from the top, and are described in Section 5.3.2. Finally GPS position information is used during data processing to synchronize the data from different experiments. The GPS velocity signal is used for vehicle speed sensor calibration. These signals enter the grade estimator from below in the figure, and are further described in Section 5.3.3. At this level

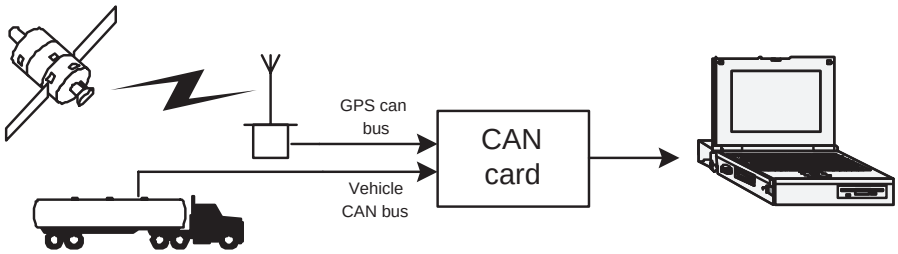

Figure 5.4: During the road tests measurement data was collected using a laptop computer with a dual channel CAN interface card. Vehicle data was logged through one of the channels, and the other one was used to collect GPS messages.

of abstraction the grade estimator has only one output, the road grade.

Experimental data was collected while the test vehicles were being driven at normal cruising speed along the highway. A laptop computer with a controller area network (CAN) bus interface card was used to log both vehicle signals and GPS data. The scenario is illustrated in Figure 5.4.

5.3.1 Grade Estimator Inputs

The vehicle speed measurements are obtained from standard CAN messages transmitted on the vehicle data bus. The measurements originate from the brake system and represent the mean speed of the wheels on the front axle. The engine torque information is sent on the vehicle CAN bus by the engine control unit. It is calculated based on the control signal governing the opening time of the diesel injectors and the current engine state. The quality of this signal is usually reasonable, although variations between individual engines, and over the life of a single engine are present. All CAN messages were logged using a vector CANCardXL (Vector Informatik, 2008) connected as shown in Figure 5.3.

Each CAN message is timestamped by the receiver board upon arrival. This timestamp has been used to synchronize all the signals during data post processing. No special consideration has been given to possibly varying latencies in the different sensors and processing units that supply the signals.

The altitude measurement comes from a single frequency (L1) GPS receiver without differential corrections. While there are higher precision GPS options available the choice of GPS receiver technology was made with regard to the belief that relatively simple receivers with similar performance to the one evaluated will be available as standard sensors in HDVs in the near future. The GPS altitude signal contains a considerable amount of noise that varies with the satellite reception conditions, as previously discussed in Section 2.4.2. For the road tests a Racelogic VBOX receiver was connected to a it's own channel on the CAN logger used to

record the vehicle CAN signals. The chosen receiver has 3D velocity measurement capabilities beyond those of regular low-cost GPS units, but the velocity outputs have not been used in this work. The specified horizontal error for the receiver is 3 m 95% Circle Error Probable (CEP) and the vertical error specification is 6 m 95% CEP. 95% CEP is defined as 95% of the measurements being within a circle of the given diameter. This absolute positioning accuracy is comparable to single channel consumer grade GPS receivers in general. The setup used does not provide any dilution of precision information from the receiver. As an effect position quality is judged only from the number of tracked satellites, as described in Section 4.1. Detailed information on the GPS receiver can be found in the user's manual (Racelogic Limited, 2008).

5.3.2 System Mode Inputs

The road grade estimator is tuned to different operating modes of the vehicle by adjustments to the assumed measurement and process noise covariances as discussed in Section 4.4. The noise covariances are determined based on the four signals entering from the top in Figure 5.3.

When the vehicle is braking the it has no accurate estimate of the torque transmitted through the wheels. The process noise for the vehicle prediction is then increased, to reduce the effects of a wrongly predicted velocity on the estimated grade.

During manual gearshifts the gearbox is briefly put into neutral and the engine is disconnected from the drive wheels. This makes our vehicle model invalid, since the reported engine torque never reaches the driving wheels. During gearshifts with the automated manual gearbox the engine is controlled to give zero torque transfer through the transmission, and the new gear is selected without using the clutch. Due to imperfections in the control during the gearshift there are often transient effects in the driveline associated with the shift, so in either case the same action is taken as during braking. The experiments $1 - 5$ were carried out using a vehicle with an automated manual gearbox, and experiment 6 was done with a regular manual gearbox. The vehicle model is updated to operate based on the newly selected gear once the gearshift is complete.

The number of tracked satellites is used together with a look-up table to determine an appropriate measurement noise covariance for the measured altitude signal.

5.3.3 Data Fusion Inputs

In order to synchronize state estimates from several runs along a road, the latitude and longitude of the current position are recorded along with each altitude value. The GPS derived speed signal is also recorded and used to calibrate the front wheel based vehicle speed. The speed measurement calibration almost completely removes wheel radius scale factor errors from the speed signal. This in turn makes

merging of data from vehicles with different stock scale factor errors much more precise. The number of satellites used to determine each position fix is saved for the measurement noise variance selection.

5.4 Data Post-Processing

After the road tests the recorded data was post-processed in order to obtain overlapping grade estimates from all experiments. The sixth experiment only produced useable data in the southbound direction, there are thus eleven one-way recordings available for analysis.

During processing the front wheel speed signal of each test vehicle was corrected using a multiplicative constant determined from the GPS speed recorded during times with good satellite coverage. The main error source in the front wheel speed is a bias due to an inaccurately assumed wheel radius. The correction constant could be determined with very low variance, and the differences in measured distance between the vehicles were almost completely eliminated. The small remaining differences in traveled distance between matching absolute positions can be attributed to slight variations in the driven path on the roadway, and possibly variations in wheel slip depending on road conditions, tires and the amount of torque transferred.

The absolute position obtained from the GPS was used to synchronize data from the different experiments. A reference point was chosen in one of the experiments, and the closest points in the data from the other experiments were then used as their respective starting points. From the starting point the traveled distance information in each experiment was used to resample all signals to a common distance vector with a 2.5 m spacing. To further reduce the error build-up in the position of the different vehicles calibration points every 10 km of the reference grade profile were used to adjust the driven distances before merging. The average distance error between the recorded reference road grade position and the recorded absolute position of a measurement point with the same distance index was 4.1 m in the southbound data set, and 2.7 m in the northbound one. With common distance indexing it was then possible to complete the road grade estimation and data fusion steps.

5.5 Road Grade Reference

The estimation results are compared to a reference road grade profile measured using an independent method. The reference profile used in this thesis has been measured using an Oxford RT3040 dual frequency high precision measurement system, that includes dual frequency GPS receiver and a tightly coupled inertial navigation sub-system based on three angular rate sensors and three accelerometers. More information about the unit can be found in (Oxford Technical Solutions Limited, 2008).

The Oxford GPS/INS system is designed to sense the 3D movements of the vehicle where it is mounted, and employs real time commercial differential GPS corrections to increase accuracy. The measurement system is specified to have a standard deviation of 0.03 % grade (pitch) and 0.1 m in the absolute position, including altitude. These specifications are for the most accurate mode, with full GPS coverage and DGPS corrections. During the test drive when the reference profile was measured the reported standard deviation in the altitude component varied between 0.3 – 0.5 m in the southbound direction, and 0.3 – 0.7 m in the northbound direction. Getting an accuracy figure for the road grade estimate is not as straightforward, but the pitch accuracy specification should be close. The suspension movement of the measurement vehicle is likely to be the major sources of error in the reference road grade, but this error has the nice property of being restricted to have a zero mean value by its physical properties. The reference road altitude and grade profile for the evaluated test segment of the road is shown in Figure 5.5.

Based on the intended primary application, look-ahead cruise control, only a low frequency reference grade profile is of interest. To obtain a suitable reference for comparison with estimation results the raw data have been low pass filtered twice, starting at each end of the data set, using a third order Butterworth filter with a spatial cut-off frequency of 0.02 m^{-1}.

5.6 Experimental Results

The proposed grade estimation algorithm shows promising results. Even if individual measurements sometimes are far from the true road grade, the merged estimate from few runs along the road comes quite close over most of the distance. The final result based on only data from the six experiments in the northbound direction and five experiments in the southbound direction, available so far, agrees very well with a reference road grade profile. Events such as braking and shifting generally decreases the quality of the road grade estimate for that experiment, but most of the time they not occur at the exact same position in all experiments. As a result of the data fusion many segments with lower quality data can be identified and suppressed in the final estimate. The main performance criterion used to evaluate the results is the Root Mean Square Error (RMSE) of the grade estimate compared to the reference road grade for that location

$$RMSE = \sqrt{E((\hat{\alpha} - \alpha)^2)} \tag{5.1}$$

This results section starts with samples of all the recorded input and auxiliary signals considered by the road grade estimator. Next comes an overview of the estimation results for all runs along the road for a representative road segment with nominal vehicle behavior. This is followed by in-depth studies of how the algorithm performs during more adverse conditions. The cases highlighted are the when the vehicle is:

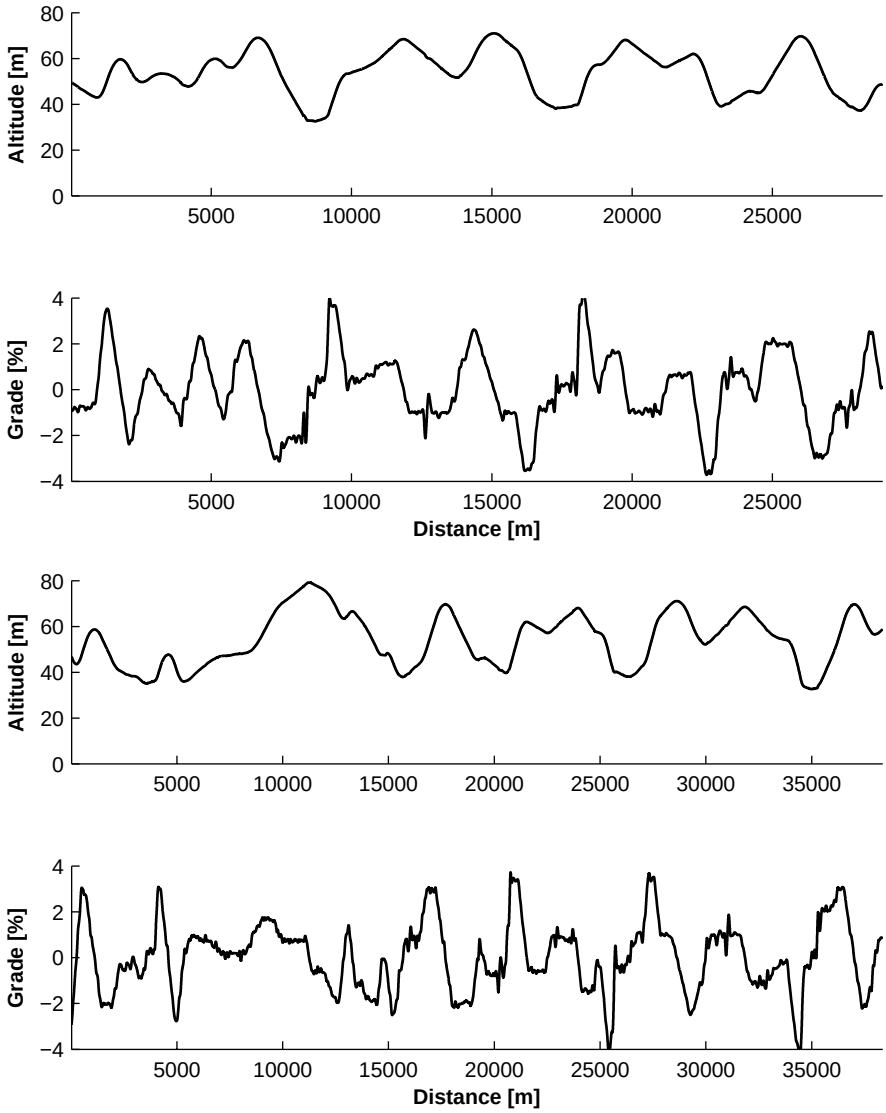

Figure 5.5: Reference altitude and reference road grade profiles for the southbound (upper two sub-figures) and northbound (lower two sub-figures) directions on the test road.

- Braking
- Shifting gears
- Losing satellite coverage

To illustrate the operation of the data fusion step in the estimation algorithm a step by step series of figures is provided. The benefits of a reduced bias in the estimated road grade from using the GPS receiver as an altitude sensor are illustrated by a comparison of estimation results when the altitude signal from the GPS receiver has been excluded from the estimation and the full input case. Finally a comparison is made between real world estimation results based on the extended Kalman filtering algorithm and the linearized system with a normal Kalman filter.

5.6.1 Sensor Data

Example sensor data recorded on a 12 km segment of the southbound test road is used to illustrate the different input signals used by the state estimator. For clarity the figures only contain data from one run along the road for each of the three test vehicles. The chosen experiments are numbers two (solid line, vehicle A), four (dashed line, vehicle B) and six (dotted line, vehicle C).

Figure 5.6 shows the recorded mean front wheel speed, GPS altitude, and engine torque. Vehicle A is heavy in relation to it's engine power, and has a typical speed profile for an economically driven HDV. The driver (or in this case the look-ahead cruise control) has ordered the speed to be lowered ahead of long downhill segments, thus reducing the amount of braking necessary. This can be seen at 15 km and 25–26 km. At 23 km the algorithm for some reason does not predict the vehicle behavior correctly, and braking becomes necessary even though the speed could have been decreased ahead of time without hitting the lower speed bound (80 km/h in this case). Vehicle B is very light, more powerful than vehicle A, and was operated with a constant cruise control system enabled. The speed profile is very flat with no speed loss in uphill segments, and no run-out in downhill segments. Vehicle C is heavy enough to gain some extra speed in downhill segment, but was following slower moving traffic for part of the drive. At 18–19 km there was a roadwork in one of the lanes, with an associated mandated speed decrease. The speed of vehicle C was controlled manually. All vehicles are electronically speed limited, and thus unable to accelerate above 89 km/h by the means of their engine. The effects of loss of satellite coverage can be seen clearly around 24–26 km in the altitude trace for vehicle B, but short signal loss also occurs with vehicles A and C. It is interesting to note the large almost static difference between the altitudes reported by vehicles B and C, and the one from vehicle A. This difference of approximately $10m$ is by no means unusual for a GPS system without differential corrections applied. The data is collected on different days, with variations in atmospheric conditions as well as the visible satellite constellation. The key advantageous properties of the GPS

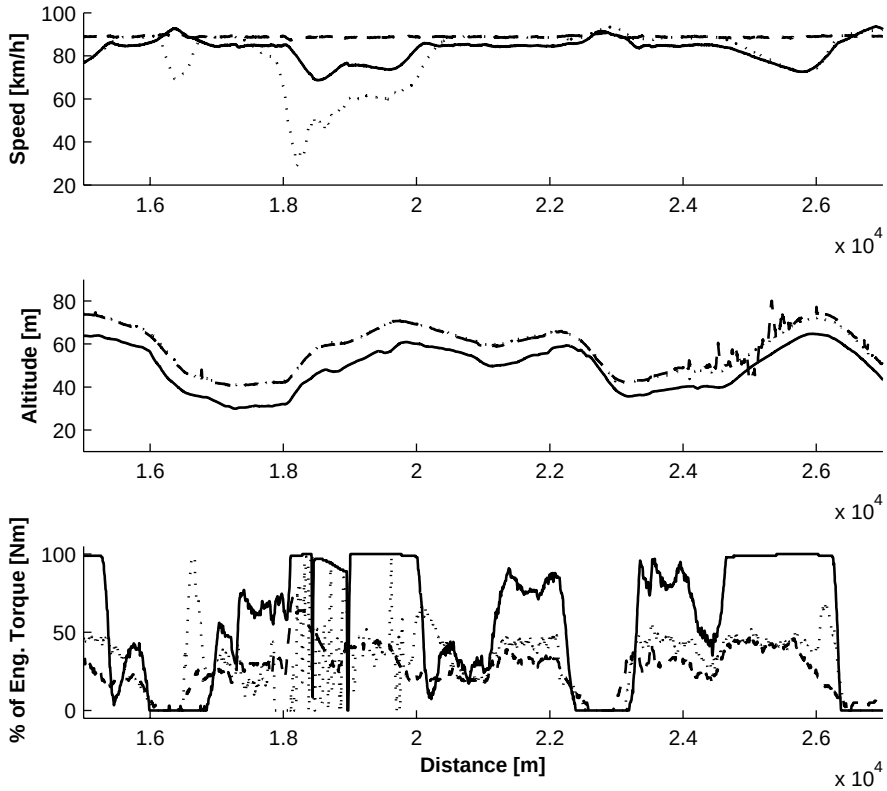

Figure 5.6: The measured states of the road grade estimator are the vehicle speed and the GPS altitude. The engine torque in the third sub-figure is treated as a known input to the vehicle model in the estimator. It is measured as a fraction of the maximum available torque for a particular engine, and then multiplied by the maximum torque. Data are shown for three runs along a road segment ranging from 15 km to 27 km in the southbound data set. The solid line represents experiment 2 (vehicle A), the dashed line is experiment 4 (vehicle B) and the dotted line is experiment 6 (vehicle C).

altitude signal is that the error changes very slowly, and that its mean is zeros over very long time periods.

The engine torque reported by the engine management system is used as an input to the longitudinal movement models for the trucks. This signal changes rapidly and is given as a percentage of the maximum torque for a given engine. It can be seen in the figure that vehicle A uses it's maximum power for long periods of time in the uphill segment, and applies no engine power in a number of downhill segments. The almost empty vehicle B never utilizes the full engine power, and rarely has a zero utilization. Vehicle C has to work slightly harder on average than vehicle B, but also shows a number of gear changes and peak power utilizations during acceleration. Gear changes can be seen in the torque data as short spikes towards zero.

The signals in Figure 5.6 are used directly in the grade estimator for time and measurement updates. In addition to these a number of auxiliary signals are used to adjust the process and noise covariances and the parameters of the vehicle model, as described in Section 4.4. Figure 5.7 shows examples of these signals. The number of available satellites is very important to the functioning of the GPS receiver, and for the equipment used the this is the best indicator of GPS altitude signal quality available. The number of tracked satellites by the same receiver can vary substantially on the same road due to the constant movement of the satellites and atmospheric conditions. This can be clearly seen in the first part of Figure 5.7, where the conditions during experiment 2 (solid line) were significantly worse than during the other two.

There are not too many gearshift available in the test data set. The cruise controller that controlled vehicle A was configured to minimize gearshifts to conserve fuel, and it was quite successful in doing so. Vehicles B and C are overpowered in the sense that they didn't need all the available engine power available on the top gear to climb the hills of the test road, and thus had no need for gearshifts. The second plot in Figure 5.7 show a segment where vehicle A needs to downshift to climb the hill, and vehicle C has to slow down and then accelerate due to the previously mentioned road work. The third plot is closely related to the second one, the shifting signal indicates when the driveline is not operating with a fixed ratio between the engine and the driving wheels. During this time the longitudinal vehicle model becomes void, and actions are taken as described in Section 4.4.

It is important to know when any of the vehicles' brakes are applied, since this leads to an external, unknown, torque entering the equations of motion. The "braking" signal indicates when the longitudinal vehicle model should not be trusted for this reason. Vehicle A applies the brakes to avoid overspeeding, while vehicle C uses them to avoid running into traffic ahead.

Finally the absolute position and vehicle velocity are recorded from the GPS for each altitude data point. This information is not used directly for the grade estimator, but it is necessary in order to synchronize several source data sets, as described in Section 5.4.

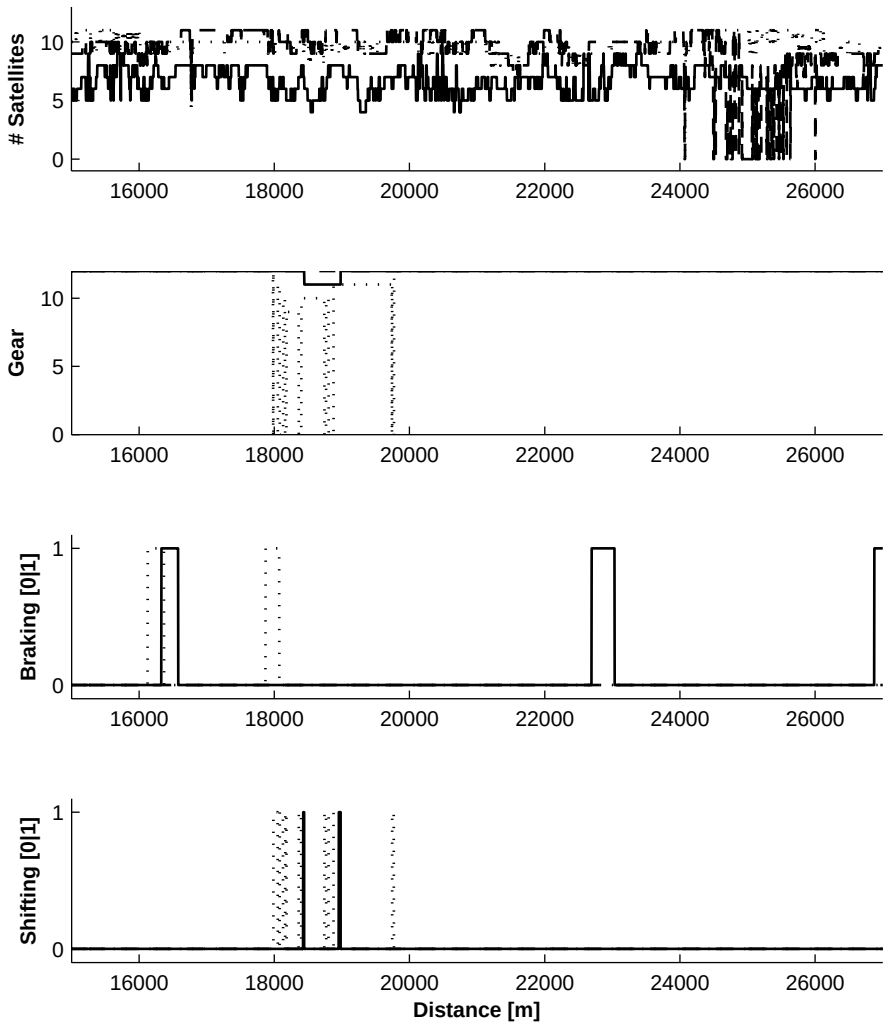

Figure 5.7: Auxiliary variables are recorded to facilitate mode switching in the filtering algorithm based on anticipated signal quality and vehicle behavior. The first plot shows the number of tracked GPS satellites, this signal is correlated with the accuracy of the GPS altitude measurements. The second plot shows the current gear. The chosen gear influences the dynamics of the vehicle model. The third and fourth plots indicate where gear shifting and braking has occurred, these events lead to adjustments in the process noise assumptions. Included are experiments 2 (solid), 4 (dashed), and 6 (dotted).

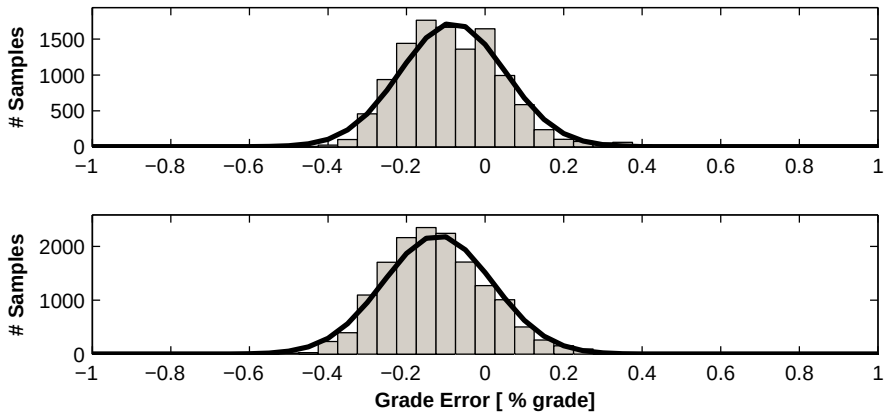

Figure 5.8: The distribution of road grade estimation errors for the southbound (top) and northbound (bottom) test roads. A normal distribution with the observed mean and standard deviation is overlaid for comparison. The observed errors are very close to being normally distributed.

5.6.2 Aggregate Results

The overall impression of the road grade estimator is that it works well and produces road grade data that should be useable for a number of applications. The estimates are not free of bias, but the inclusion of the GPS makes the results fair even when the vehicle parameters are non-ideal, as seen in Section 5.6.7. On the southbound test road as a whole the RMSE of the estimated road grade was 0.16 % grade. A relatively large part of the error was du to a bias of −0.08 % grade. For the northbound direction the RMSE was 0.18 % grade, with a bias of −0.12 % grade. The statistical distributions of estimation errors in the two test roads are illustrated in Figure 5.8, together with normal distributions with the same standard deviations. It can be seen that the errors are roughly normally distributed, with the identified bias.

There is a medium to high correlation between the road grade estimation errors and the rate of change in the road grade. When the road grade changes rapidly, the estimation error increases. This is caused by an apparent misalignment of the reference road grade profile by approximately 12 m. The estimated road grade profile changes at an earlier position along the road than the reference grade profile. This effect may be depend on the way the filtering and smoothing steps of the estimation method works, or on some timing issue in the data processing. The 12 m difference amounts to about 0.5 s at highway speeds. With knowledge of the reference grade, the misalignment can be corrected retroactively by finding the distance offset that minimizes some performance criterion, e.g. the RMSE in the

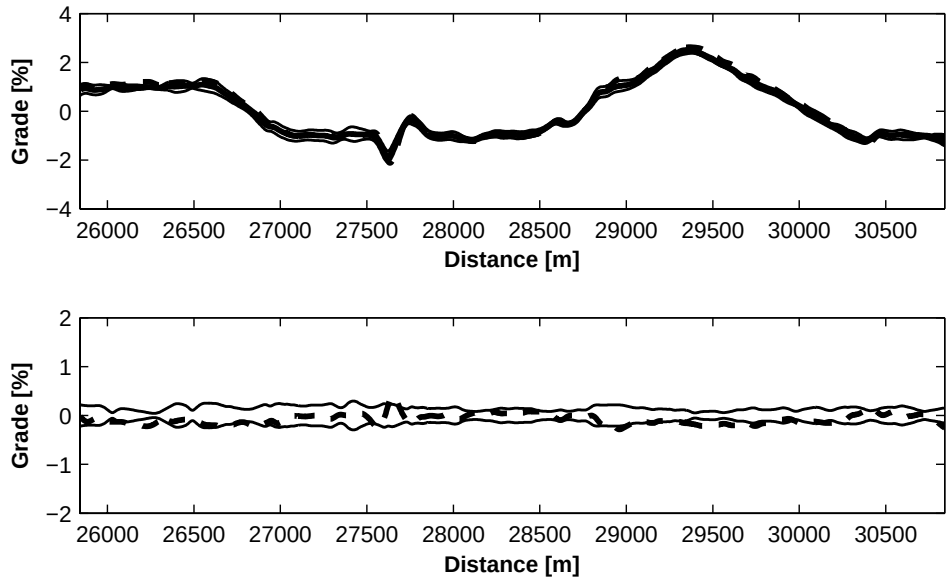

Figure 5.9: The top figure shows the final grade estimate calculated through data fusion based on six experiments (solid). It agrees well with the reference grade profile from a specialized measurement vehicle (dashed). The numerical one standard deviation interval around the final grade estimate at each sample point, based on the six experiments, is also shown (thin lines). The bottom figure shows the difference between the fused grade estimate and the reference profile (dashed), as well as the standard deviation from the top figure (solid).

grade estimate. Doing so eliminates the mentioned correlation and reduces the road grade RMSE by approximately 0.2 % grade, but also sacrifices the ability to apply the complete method without access to a road grade reference. It has been opted not to correct the alignment in the analyzed data at this time.

To illustrate the magnitude of the obtained estimation errors during nominal driving the numerical standard deviation among the six road experiments on the southbound road is investigated. Figure 5.9 shows the agreement of the final grade estimate with the reference for a 5 km segment of the southbound test road, together with the sample standard deviation for each data point.

5.6.3 Braking

One of the most challenging situations for the grade estimator is when the vehicle applies one of the brake systems. Therefore, we shall study one such occasion in

more detail. During braking the engine will generally report a negative net torque from internal friction when fueling is cut off. This means that the vehicle model based prediction in the grade estimator will be computed using only the engine friction as its driveline input, even though there is a braking force present as well. The roll resistance and air drag will still be correctly modeled. The missing brake force will then be attributed to the gravity component, aka the road grade. This should lead to a road grade estimate that is too high (more uphill than in real life). In order to avoid this effect, and at the same time raise a flag to the data fusion algorithm that this data deserves lower trust than the norm, the process noise covariance for the velocity state is increased. This causes the estimator to rely less on the vehicle model, and more on past road grade estimates and the GPS measurements. At the same time the estimated error covariance of the output increases.

The example segment shown in Figure 5.10 represents a comparatively steep downhill segment, where the heavy vehicle A needs to apply the brakes to avoid exceeding its set maximum allowed speed. Data is shown for experiments 2 (solid, vehicle A), 3 (dashed, vehicle A), and 6 (dotted, vehicle C). Vehicle C does not apply the brakes in this segment. Figure 5.10 shows the key signals of interest during braking. The first two sub-figures show the velocity profiles and GPS altitude measurements, after that comes the reported engine torque and braking signal. Vehicle A is pulled down the hill by its weight, and does not need to utilize the engine until the very end of the segment. Vehicle C, at 21 tons, can only coast at a constant speed for a few hundred meters, and then needs to use engine power to maintain speed. Braking is required by vehicle A for a total of almost 1 km in each of the experiments. The resulting road grade error in the fifth part of the figure shows that experiment 2 yields an overestimate of the grade during the first brake application, an underestimate during the second, and no visible additional error during the third application. Experiment 3 yields no significant additional error during the first application, and overestimates of the grade during the second. The final part of the figure shows the estimated grade error covariance after the smoothing step in the grade estimator. The estimated error variance almost doubles during the segments where the brakes are applied.

Somewhat surprisingly the experimental data does not indicate that the investigated periods of braking severely affect the overall merged road grade estimate. Figure 5.11 shows the RMSE values for the road grade for each experiment, as well as for the map based on an increasing amount of data. The road grade RMSE of the entire segment is compared to the RMSE for only those sample points where the vehicle was braking in at least one of the experiments. Braking occurred primarily in vehicle A. This led to an increased estimation error for most of the corresponding experiments. The worst effects were seen in experiment three, with vehicle A. This was also the experiment that showed the highest errors over the entire segment, out of those done with vehicle A, as indicated by the third star in the figures. Given that the same vehicle was used for experiments $1-3$ this indicates that the weather conditions were less in agreement with the parameters used on the day of the third

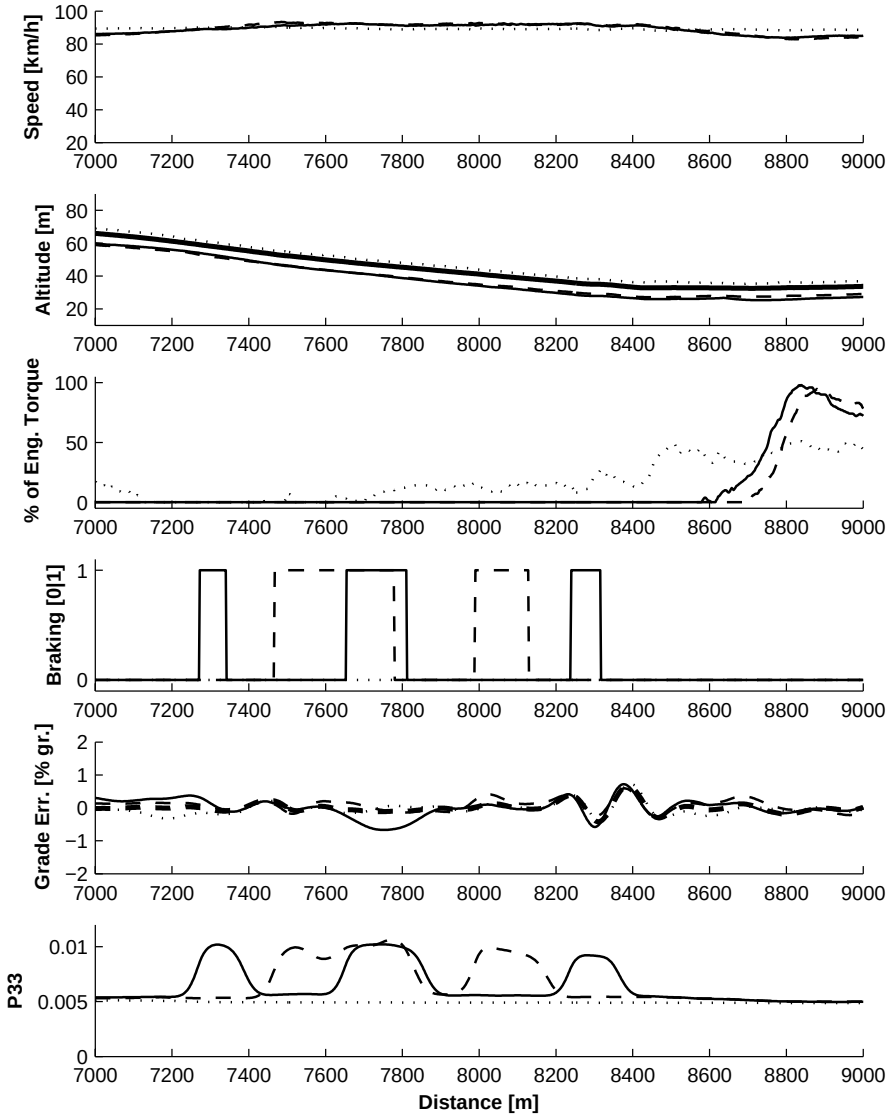

Figure 5.10: Signals of interest during braking for a segment of the southbound test road. Data is shown for experiments 2 (solid), 3 (dashed) and 6 (dotted). In the fifth part the road grade error of the merged final estimate is shown as well (thick solid).

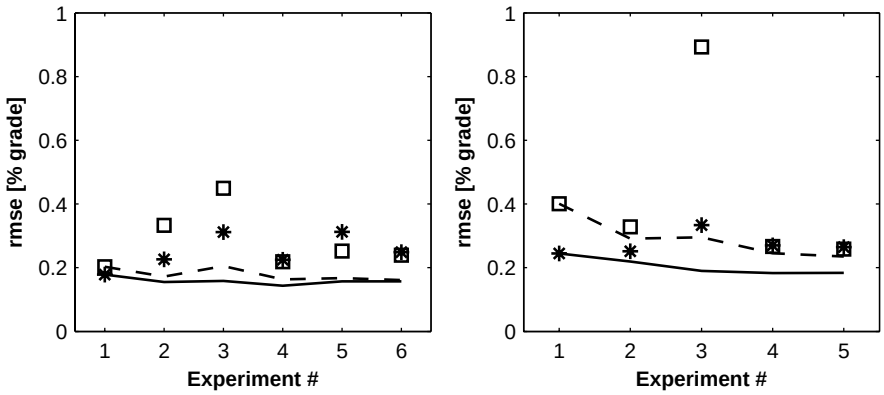

Figure 5.11: Estimation results during braking. The road grade estimate RMSE is shown for the southbound (left figure) and northbound (right figure) test segments. The value for the entire road segment, based on the experiments up to and including the index on the x-axis, is shown (solid line) together with the value when only the sample points where braking occurs in at least one experiment are included (dashed line). The values for the individual experiments are shown with stars for the entire segment and squares for the sample points corresponding to the dashed line.

experiment that for the previous two. A brake system was engaged in at least one of the experiments in the southbound data set for a total of 2518 m. For these parts of the road the RMSE in the road grade estimate was the same as the total average of 0.16 % grade. In the northbound direction the effect was more noticeable. A brake system was used in some vehicle for a total of 1568 m. At these times the RMSE increased from 0.18 % grade for the entire road segment, to 0.24 % grade.

In the current implementation of the grade estimator there is no way of assessing the amount of brake torque being applied. If the driver uses the retarder or engine brake as opposed to the wheel brakes there is a possibility to have some additional information on the magnitude of the force.

5.6.4 Shifting Gears

During gearshifts the engine is disconnected from the rest of the driveline, and the model for the influence of the engine torque becomes void. This is handled by setting the engine torque input in the grade estimator to 0 while the status signal ”Shifting´´ is active. The friction losses from the driving wheels to the disconnected gearbox are assumed to be negligible. After the gearshift the estimation continues, with a vehicle model suitable for the newly chosen gear. A shift of gears introduces quite a lot of non-linear and oscillatory behavior in the driveline, that is not captured by the model used. To attempt reduce the negative impact of these effects

in the merged estimate the process variance for the velocity prediction is increased during the gear shift in the same way as during braking.

Example data for a segment with many gear shifts is shown in Figure 5.12. The segment chosen to illustrate the behavior during gear shifts contains a 2 km long uphill segment, that is steep enough to require downshifting in vehicle A. During the experiments with vehicle C there was a road work set up at this location, leading to slow moving traffic, as seen in the first part of the figure. The third and fourth parts of the figure show the shifting signal and the current gear. The gear shifts in the two experiments with vehicle A occur close to each other, but do not overlap. The fifth part of the figure shows the road grade estimation error for the three studied experiments, as well as for the final grade estimate. It can be seen that the estimation error generally increases somewhat during the gear shifts. Right before the 19 km mark the estimation error increases significantly during the upshifts for vehicle A. This can be explained by a large error in the derivative of the GPS altitude measurement at that location, as seen parts four and five of Figure 5.13. As the process variance of the vehicle model is increased during the gear shift, the influence of the GPS signal grows. There is a fair number of satellites being tracked at the location, and thus the GPS altitude derivative affects the estimation results.

The large error in all the estimates, and the merged result, around 18 km is due to the algorithm finding the start of the uphill segment at an earlier position than it occurs in the reference profile, as seen in part two of Figure 5.13. The drop in the base level of $P_{(3,3)}$ in the fifth part of Figure 5.12 for vehicle C is explained by a drop in the measurement innovations during the time. The Q and R matrices are only adjusted during the shift events. 5.13.

Overall gear shifts, or the driving conditions where gear shifts are performed, yielded mixed grade estimation results. Figure 5.14 shows the RMSE values for the road grade for each experiment, as well as for the map based on an increasing amount of data. The road grade RMSE of the entire segment is compared to the RMSE for only those sample points where the vehicle was shifting gears in at least one of the experiments. The road segments where shifting occurred in some of the experiments generally gave worse estimation results than the test road as a whole. Again, in the same way as during braking, the third experiment was particularly severely affected. However, gearshifts took place in experiments 1, 2 and 6 as well, so gearshifting does not always yield bad grade estimates. In the southbound data set at least one of the vehicles indicated shifting status for a total of 595 m. During this time the road grade RMSE rose to 0.26 % grade, from the 0.16 % grade result for the entire segment. In the northbound direction shifting was indicated for only 218 m. This lead to a road grade RMSE of 0.15 % grade, compared to 0.18 % grade for the entire data set.

5.6.5 Low Satellite Coverage

While there are very few occasions in the test data where the GPS satellite reception is completely blocked, there are a few instances where signal blockage and/or

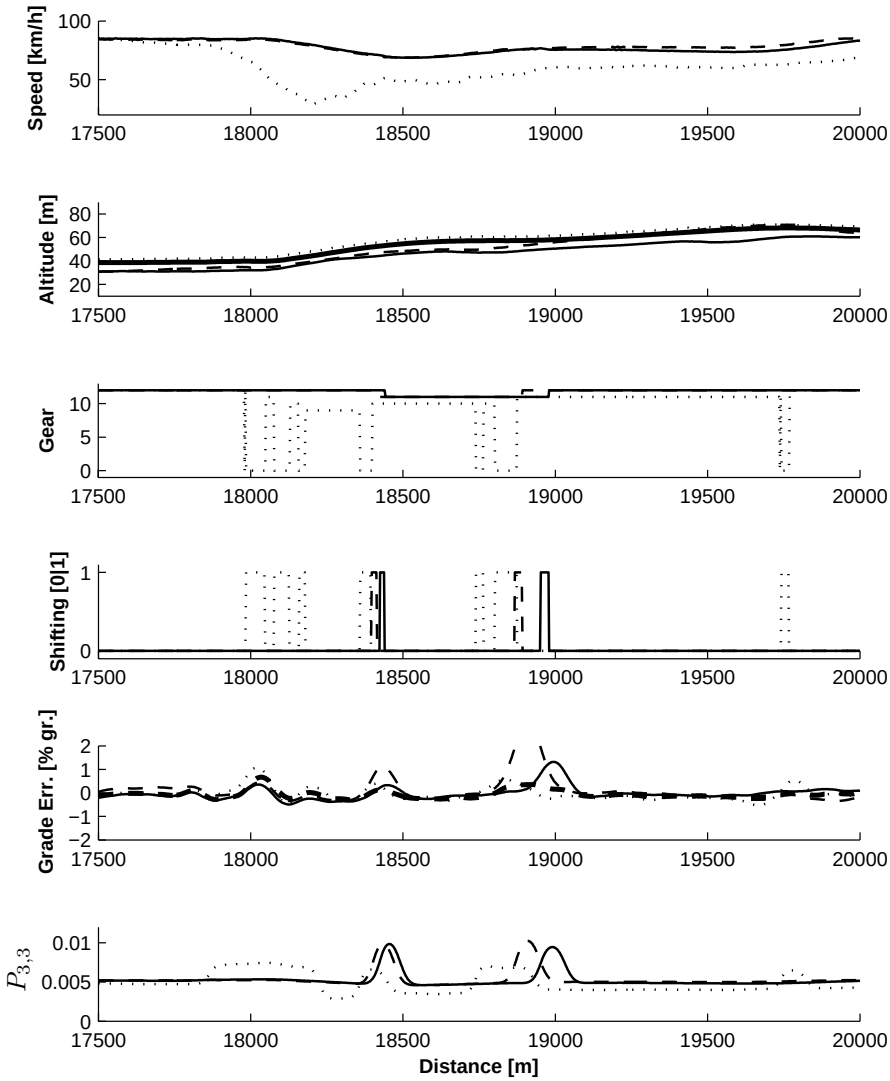

Figure 5.12: Road grade estimation results during gear shifts. Data is shown for experiments 2 (solid), 3 (dashed) and 6 (dotted). In the second part the reference altitude is also included (thick dashed), and in the fifth part the road grade error of the merged final estimate is shown (thick solid).

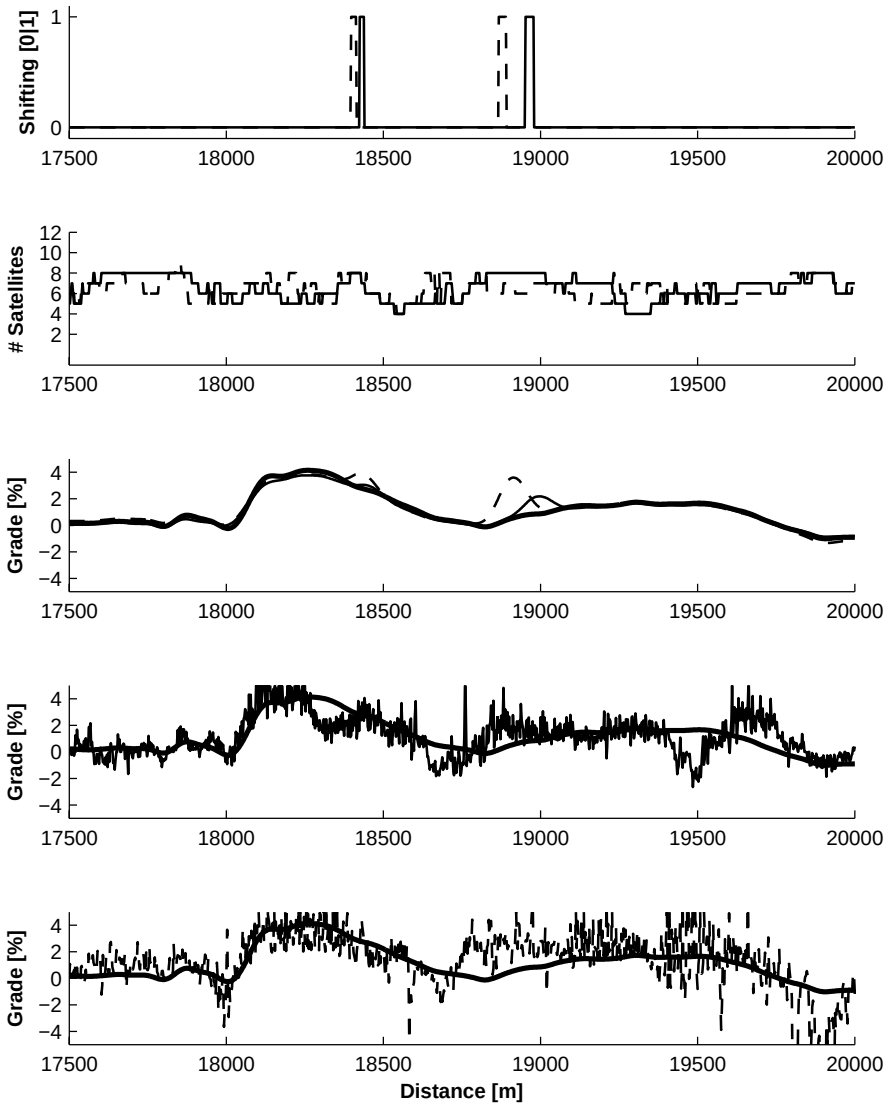

Figure 5.13: The shift signal and GPS data are shown for experiments 2 (solid) and 3 (dashed). The reference grade (thick solid) is included in parts three-five. Parts four and five show the numerical derivative of the GPS altitude for experiments 2 and 3 respectively. The altitude derivative has a significant difference to the reference road grade during the second gear shifts before the 19 km mark.

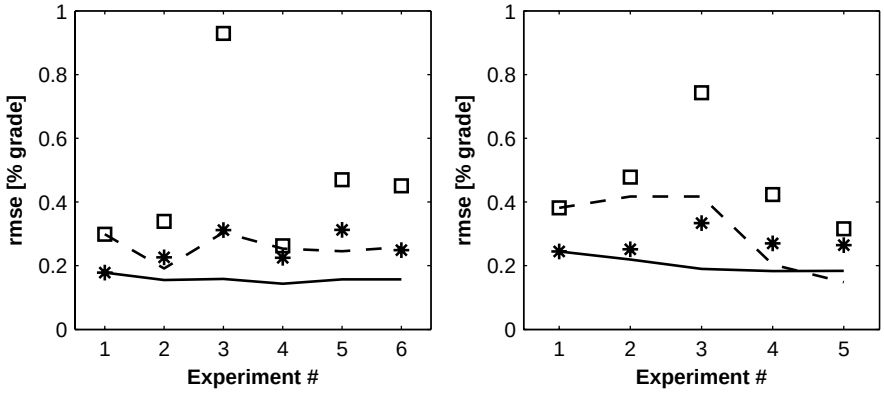

Figure 5.14: Estimation results during gear shifts. The road grade estimate RMSE is shown for the southbound (left figure) and northbound (right figure) test segments. The value for the entire road segment, based on the experiments up to and including the index on the x-axis, is shown (solid line) together with the value when only the sample points where shifting occurs in at least one experiment are included (dashed line). The values for the individual experiments are shown with stars for the entire segment and squares for the sample points corresponding to the dashed line.

multipath effects causes significant degradation of the altitude data accuracy. The effects can be seen in the GPS altitude data on the road segment shown in Figure 5.15. The 1.5 km segment contains a hilltop where the GPS signal is obstructed in several of the experiments. In part two of the figure it is evident that the GPS altitude signal for experiments 2 and 5 contains an unusually large error component. Looking at the number of tracked satellites we note that very few satellites are being tracked in both experiments 2 and 3, yet experiment 3 seems to be much less adversely affected. When three or fever satellites are tracked the GPS altitude data is disregarded entirely, four or five tracked satellites lead to a very low trust in the data. The number of tracked signals in experiment 5 should be adequate for a reliable 3D position fix, yet the altitude signal is very noisy. From the observation data it seems likely that there are severe multipath problems with reflected signals in this segment. This indicates that it would be desirable to use more diagnostic data about the GPS receiver state in addition to the number of tracked satellites. The raw GPS altitude is treated by a simple outlier detection scheme the maximum change between two consecutive measurements is restricted to 1 m (corresponds to a road grade of 40 %) before it is fed into the road grade estimation.

To make the estimation task even harder, experiment 2 includes gear shifts during the satellite signal outages around 1600 m and 1900 m, as seen in part four.

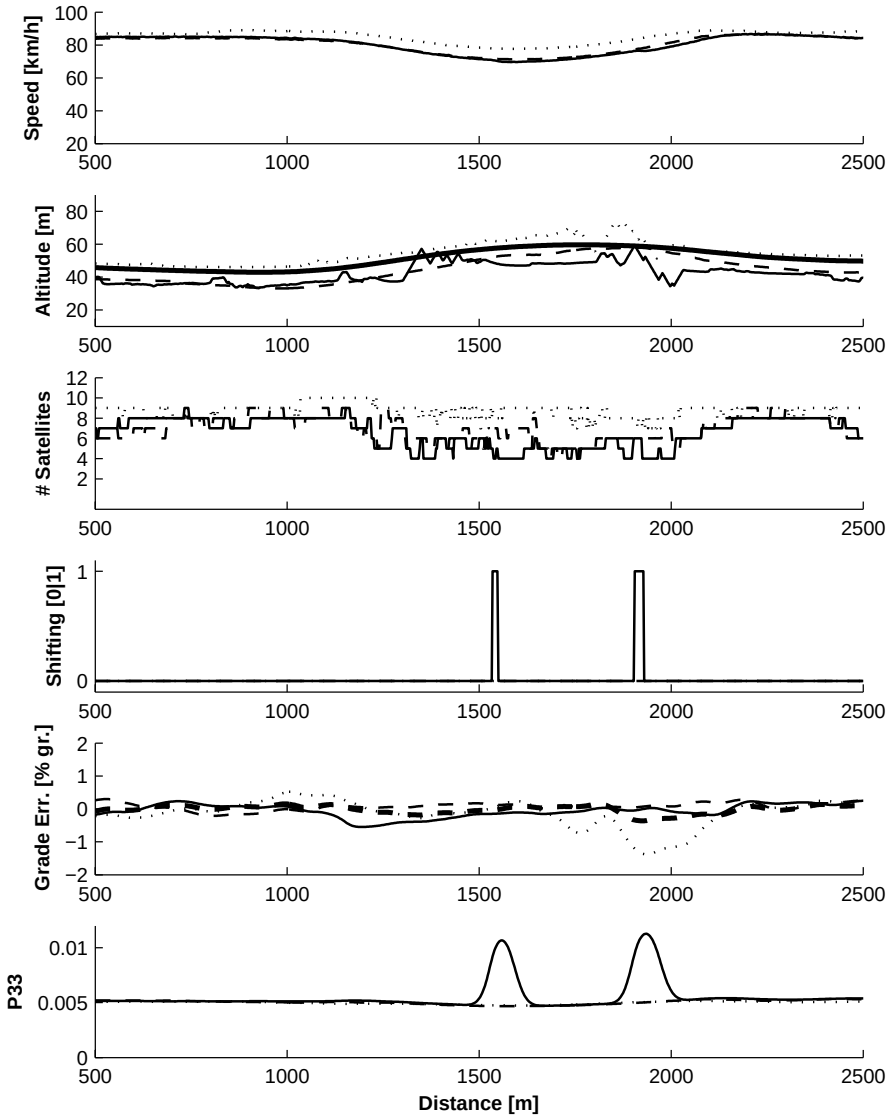

Figure 5.15: Road grade estimation performance during loss of satellite coverage. Several of the experiments show unusually high GPS altitude noise in this segment. Data is from experiments 2 (solid), 3 (dashed) and 5 (dotted). In part two the altitude reference is included (thick solid), and in part five the merged road grade error is shown (thick dashed).

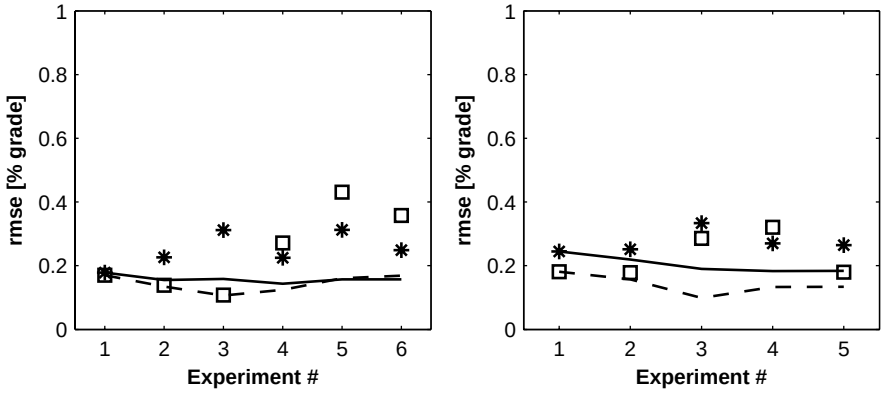

Figure 5.16: Estimation results during loss of satellite coverage. The road grade estimate RMSE is shown for the southbound (left figure) and northbound (right figure) test segments. The value for the entire road segment, based on the experiments up to and including the index on the x-axis, is shown (solid line) together with the value when only the sample points where there is no satellite coverage in at least one experiment are included (dashed line). The values for the individual experiments are shown with stars for the entire segment and squares for the sample points corresponding to the dashed line.

During the gearshifts there is no trustworthy data coming from either of the sensors, this immediately leads to large grade estimation errors. These errors are somewhat mediated in the data fusion step, since the gear shifts lead to raised estimated grade error covariances. However, the GPS altitude noise in experiment 5 also leads to a high error in this grade estimate. Since there are many satellites being tracked this error is not detected and flagged in the R matrix. As noted in 4.4 increases in GPS altitude measurement noise does not influence the estimated error covariance for the road grade state by any noticeable amount, due to saturation. This explains the lack of variation of $P_{(3,3)}$ in the sixth part of Figure 5.15.

The experimental data only contains short segments of total loss of satellite coverage, in the northbound direction it only occurred in at least one experiment for 313 m. For those grade estimates the satellite signal is effectively left out of the filter, and it consequently does not matter if the signal is very noisy. Figure 5.16 shows the RMSE values for the road grade for each experiment, as well as for the map based on an increasing amount of data in the same way as for the braking and shifting events. The road grade RMSE of the entire segment is compared to the RMSE for only those sample points where satellite coverage was lost in at least one of the experiments. There is no indication that the total grade estimate on the average should be any worse where there are problems with the satellite reception.

This is reasonable since the main effect of the altitude signal, at least while the vehicle model operates normally, is to provide bias compensation. During short outages the grade bias component does not have time to grow enough to cause a noticeable degradation of the estimates. In the southbound data set at least one of the vehicles indicated loss of satellite coverage for a total of 1328 m. During this time the road grade RMSE was largely unchanged at 0.17 % grade, compared to the 0.16 % grade result for the entire segment. In the northbound direction loss of coverage was indicated for 313 m. This lead to a road grade RMSE of 0.13 % grade, compared to 0.18 % grade for the entire data set.

5.6.6 Iterative Data Fusion

Using data from more than one run along the road and more than one vehicle improves the reliability of the final grade estimate. The downhill segment from $s = 22150$ m to $s = 23150$ m is one of the hardest parts of the test road to estimate accurately, it is therefore used as an example of how the data fusion step improves the quality of the final grade estimate. The grade maps resulting from the progressive inclusion of data from the six experiments can be seen in Figure 5.17. As more data is added the road grade map is improved. The mean value of all included grade estimates at each sample point is also shown, to highlight the effect of the data fusion step. Each figure shows the latest experiment (dashed), the road grade map based on all experiments added so far (solid) and the reference road grade (dotted).

Figure 5.18 shows a comparison of the smoothed estimates from all six southbound experiments with the final grade estimate and the reference grade profile.

5.6.7 Vehicle Model Bias

Without the GPS altitude measurements the vehicle model and measured signals give an estimated grade that has a bias due to modeling errors. The bias is reduced when the GPS altitude measurement is introduced as a vehicle independent low frequency correction in the filter. Depending on the vehicle parameters the magnitude of the drift varies. Figure 5.19 shows the estimated grade and altitude when the grade estimator has been operated without GPS input data. Table 5.2 shows the mean grade biases observed in each of the experiments when compared with the road grade reference. The grade biases range from negligible for vehicle A (experiments 1–3), when using the GPS, to severe for vehicle B (experiments 4–5). It is evident that results could be improved if the parameters for vehicles B and C were better calibrated to match the vehicles and environmental conditions they are supposed to describe.

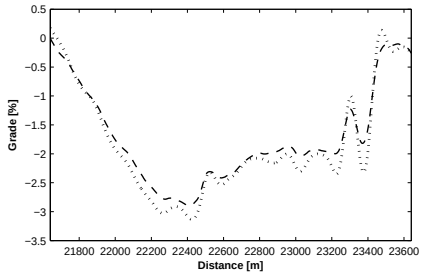

(a) The first experiment forms a road grade map by itself. Estimation errors cause it to differ from the reference road grade.

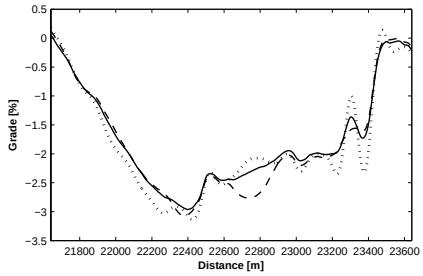

(b) When a second experiment is added to the one in (a) a new road grade map is obtained. The large disturbance in experiment two at $s = 22100$ m has high uncertainty and thus a low weight in the data fusion.

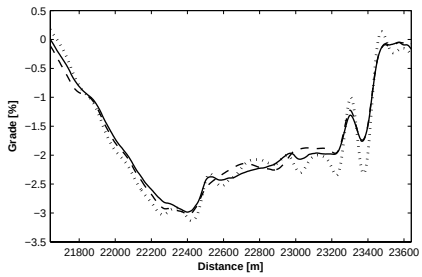

(c) The third estimate from vehicle A does not differ much from the map based on the previous two runs along the road.

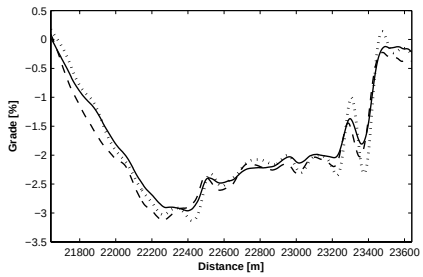

(d) The larger difference in the fourth estimate is probably due to different model parameter errors in relation to vehicle B.

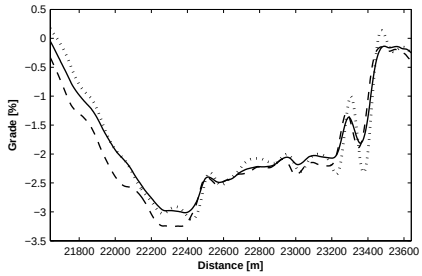

(e) Estimate five is based on vehicle B, just like the one in (d).

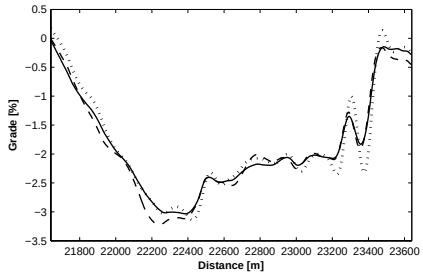

(f) When the sixth estimate, recorded with vehicle C, has been added the map is complete.

Figure 5.17: Iterative road grade estimation results after each iteration. In each figure the most recently added experiment (dashed), is shown together with the reference road grade profile (dotted) and the merged estimate based on all experiments added so far (solid).

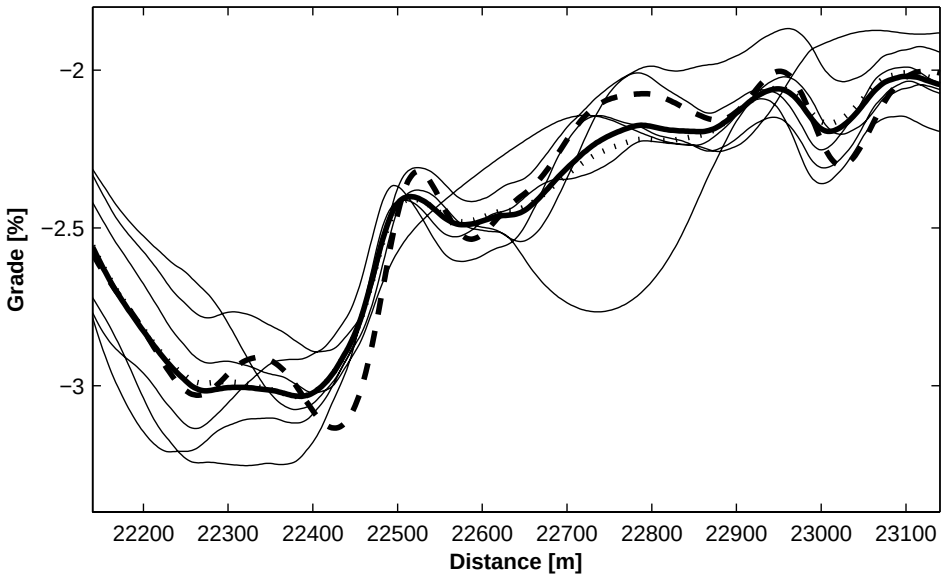

Figure 5.18: The final merged road grade estimate (solid) is shown with the reference grade profile (dashed) and the mean value of all smoothed estimates (dotted). The estimates from the individual experiments are also included (thin lines). This is a magnification of the most challenging part of the test road. The estimate based on experiment two is particularly at odds with the rest at 22750 m. This is due to a combination of poor satellite coverage and the effect of the braking. The detrimental effect on the fused estimate is smaller than on the mean.

5.6.8 Linear System Model

The results from using the piecewise constant linear model instead of the time-varying non-linear model indicated only marginal changes in the estimated road grade. A comparison of road grade estimates obtained with the two methods is shown in Figure 5.20. The main non-linearity in the vehicle model, for the magnitude of road grades considered, is in the speed. The linear model is only valid for velocities close to the linearization point of 80 km/h. During most of the experiments the speed of the measuring vehicle was close to this value. The proposed method is primarily suited for highway estimation, and it would probably be wise to reject any data sets with large speed deviations, regardless of whether the linear or non-linear model is used.

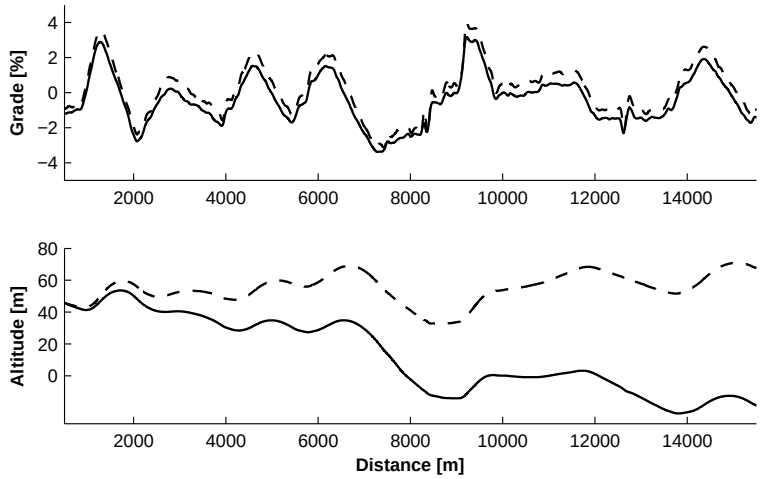

Figure 5.19: The top part of the figure shows the estimated road grade without the GPS input (solid). This signal lies significantly below the reference profile (dashed). As a result the altitude estimate has a significant drift. Since there is no absolute altitude measurement available in the filter it is initialize to the same starting value as the reference profile.

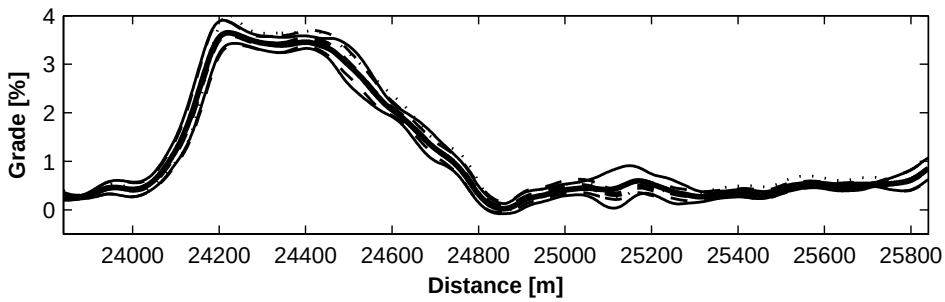

Figure 5.20: The final grade estimate based on the non-linear model (solid) with confidence interval (thin lines) is shown together with the one based on the piecewise constant linear model (dashed). The reference grade is also shown (dotted thin line). The differences between the two methods are slight, and significantly smaller than the deviation from the reference grade.

Table 5.2: Observed mean bias in estimated road grade, with and without GPS input, for the south- and northbound test roads. The road grade figures are given in percent

Direction	Meas.	Vehicle	Mean bias w. GPS	Mean bias w/o GPS
South	1	A	-0.02	-0.15
South	2	A	-0.04	-0.18
South	3	A	-0.03	-0.34
South	4	B	-0.12	-0.88
South	5	B	-0.18	-1.28
South	6	C	-0.09	-0.58
South	Merged		-0.08	-0.57
North	1	A	-0.09	-0.54
North	2	A	-0.10	-0.58
North	3	A	-0.06	-0.57
North	4	B	-0.17	-1.31
North	5	B	-0.17	-1.30
North	Merged		-0.12	-0.86

5.7 Summary

Experimental data have been collected in a total of eleven experiments using three HDVs on a Swedish freeway. The six data sets from the southbound segment and the five from the northbound segment have been merged into two road grade maps. The road grade estimates based on the proposed method have been compared to a reference road grade profile obtained using specialized equipment. Overall the performance of the proposed method is promising, even though vehicle model or parameter errors cause a slight bias in the estimated grade. The estimation error increases during braking, but the error in the final estimate based on experiments where braking takes place at different locations is not affected as much. The analysis of estimation performance during gear shifts yielded mixed results. Data points where gear shifts occur in at least one experiment showed higher than average errors, but this did not seem to be entirely due to the gear shifts. Temporary loss of satellite coverage did not cause any consistent effects on the road grade estimate. Finally it was noted that the GPS receiver is vital to bias rejection, some experiments showed severe bias in the estimated road grade when the estimation was carried out without it. Grade estimates based on the linearized model showed comparable results to those obtained with the nonlinear model.

Chapter 6

Conclusions and Future Work

It has been shown through experiments that the proposed road grade estimation algorithm generates results that are consistent with the reference grade profile for the road. The usage of both the vehicle model and the GPS altitude sensor improves the estimates beyond what would be possible to achieve using only one data source. The inclusion of data from more than one run along a road segment safeguards against spurious errors penetrating the road grade map. This chapter details the conclusions that can be drawn from the results, and outline avenues for future work in the area.

6.1 Conclusions

Recent advances in the development of embedded electronics and low cost global positioning enable new vehicle control systems that use map data to supplement traditional sensors in building a model of the surroundings. These systems rely on digital maps that include accurate road attributes. We have seen that the road grade is an attribute of particular importance to many HDVs, and that the required road grade maps are not currently at hand. A system model has been developed, that links the road grade to sensor signals that are generally already available in the control network of vehicles with map enabled ADAS. Using this system model an iterative method for creating and improving road grade maps has been created. The method uses information about gear shifts, vehicle braking and satellite coverage to adapt the grade estimator and weight the influence of new grade estimates being added to the map. Experimental results have shown that the combination of in-vehicle sensed signals with GPS receiver derived altitude generates a road grade estimate with a higher and more consistent accuracy than each of the sensors taken by themselves.

The proposed method for grade estimation combines the long term stability of the GPS derived altitude signal with the short term smoothing and dead reckoning capabilities of the vehicle model based grade estimation. The inclusion of the GPS receiver counteracts much of the bias in the grade estimate introduced by vehicle

model, and vehicle model parameter, errors. On the other hand the vehicle model is able to capture short term variations in the road grade much better than what would be possible using only the noisy derivative of the GPS receiver altitude signal.

The grade estimator based on a piecewise stationary linear vehicle model performs similarly to the one utilizing a time-varying non-linear model. This opens up possibilities both to lower the computational requirements and to gain more insight into how the filter can be improved, based on results for optimal filtering of signals generated by linear systems.

Experiments have shown that already at this stage the proposed method is feasible for collecting road grade with an average RMSE of 0.17 % grade for the two test roads. Braking, gear shifts and loss of satellite coverage are handled well when they occur simultaneously only in some of the included experiments. Previous practical experience, as well as a theoretical analysis, show that road grade estimates of the obtained quality are useable for example in a look-ahead cruise controller based on road grade data.

6.2 Future Work

The performance of the road grade estimator developed so far shows that using data from multiple runs along a road as a way of generating accurate road grade estimates based on standard HDV sensors is feasible. During the project a number of areas have been identified, where further exploration might lead to improved performance. These ideas are presented divided into three categories. Improvements to the road grade estimator itself are given first. This is followed by a discussion on possible additional sensors and better usage of the current ones. Finally, enhancements relating to the use of multiple vehicles and more data from additional runs along the road are treated.

6.2.1 Grade Estimator

The road model currently used in the grade estimator includes no dynamics for the road grade state. As a consequence the process noise of the road grade state has to be set large enough to accommodate the changes in the grade that are caused by the road designer, as described in Section 3.2. This is true regardless of the amount of changes in the road grade estimate actually originating from the road, and the amount that comes from noise and measurement errors. A hybrid estimation scheme that uses multiple road models and allows for discrete changes in the vertical curve radius might be useful in identifying the road grade profile specified by the road designer. Nevertheless, there are most likely differences between the designed road grade profile, with clearly delimited segments with specified vertical curve radii, and the actual road. It is therefore an open question whether this would yield a better estimate of the true grade than the current method.

It would be interesting study ways to improve the current ad-hoc process for selecting the Q and R matrices. This could for example be done through some

adaptive filter that estimates the noise characteristics at the same time as the system state. Another possibility would be to select the matrices based on some performance criterion for the grade estimator.

A closer look at the sensors and how they are modeled may enable their noise characteristics to be estimated and used directly in the Kalman filter, in place of the design parameters currently used. This can either be done off-line, to provide better design parameters, or on-line during operation of the estimator. With the true sensor noises available, estimation of the magnitude of the process noises for the linear version of the vehicle model may also become a possibility. Ideally this would lead to greater confidence that the grade estimator is operating in the best way possible at any given time.

The current weighted average data fusion approach can most likely be improved by using more advanced techniques. Various kinds of formulations of distributed Kalman filters, e.g. the Kalman filter on information form could be investigated for this purpose. The key issue is to retain the distributed property in the sense that the storage space required for a particular road segment should not increase as data from additional runs along the road are processed and included in the road grade estimate.

As more estimates are added to the road grade map the need for automation in the data handling process increases. Before an autonomous road grade estimator can be implemented in a production vehicle the issue of automatic road map generation has to be solved. This road map can then be augmented with the estimated road grade. This is a challenging multi-disciplinary task for the future. A step on the way to completely autonomous operation would be a solution where individual vehicles transmit their sensor information to some central processing location where human operators can assist in the map building.

The piecewise linear model for the vehicle, and the resulting grade estimator, have primarily been tested on the highest gear, since most of the data currently available is captured in this mode. The linearization points to choose for optimum performance, and the effects of frequent mode switching between the various linear models need to be examined further. Using the linear model it might be possible to more formally examine the convergence limits for the road grade estimator. One result could be a bound on the amount of switching between linear models that can be handled without risking to loose convergence in the estimator.

6.2.2 Sensed Signals

In the current implementation of the road grade estimator the filter variance for the altitude measurement noise is set from a look-up table based on the number of tracked satellites. While the number of tracked satellites can correctly signal when the altitude measurement is completely useless, i.e. too few tracked satellites for an altitude fix, the converse is not entirely true. There may be significant altitude errors present even though an adequate number of satellites are being tracked. Most GPS receivers supply a vertical dilution of precision signal that can be used to get

an idea of the size of the part of the error in the altitude signal that is the result of bad satellite geometry. This information could be used to improve the estimate of the altitude sensor noise. The equipment used in this study did not provide such a signal, so it's usefulness has not yet been tested.

As of now, the only signal directly fed into the filter in the grade estimator from the GPS receiver is the altitude measurement. The latest generation of low-cost integrated GPS receivers provide direct measurements of 3D velocity in addition to position estimates. This capability opens up an interesting avenue to possibly improve the road grade estimate based on inclusion of the instantaneous GPS derived grade estimate available through the ratio of vertical velocity to longitudinal velocity. Whether the GPS velocity measurements contain any useful new information compared to what is already available through the vertical position measurement remains to be investigated.

It is likely that an increasing number of HDVs will be equipped with accelerometers for determining the longitudinal acceleration. In an incline this device will experience an acceleration due to the horizontal component of the gravitational force. The vehicle acceleration determined from wheel sensors or from the GPS receiver will not include this component. The difference between the acceleration estimates can then be used to assess the road grade, and provide further input to the combined grade estimate.

The distributed nature of the road grade estimator allows for it to be used with more than one vehicle. If there is a communication channel available, with other vehicles or with the home office, the vehicle could exchange map data with others. A fleet owner for example could download all the map data from all vehicles in the fleet, and thus build accuracy and coverage in the aggregate map much faster than if every vehicle is left to fend for itself.

6.2.3 Robustness to Vehicle Parameters

It can be seen from the results when the grade estimator is run without GPS receiver input that the road grade estimation bias caused by errors in the vehicle model or vehicle parameters differs significantly between the different vehicles. This indicates that better overall performance might be achievable by closing the loop and estimating the vehicle parameters as well. Previously published studies of GPS receivers and vehicle models in road grade estimation indicate that at least the vehicle mass should be identifiable during periods of good GPS coverage.

To further develop and tune the algorithm it would be desirable to have access to a larger set of experimental data. Since a typical HDV in long haulage operation travels the same routes very frequently, dozens of estimates for the most important road segments will many times be available quite quickly. A larger field study with more runs along each road segment would thus enable a better prediction of the final accuracy achievable by the method.

Bibliography

ISO 11898-1:2003. 2003. *Road vehicles – Controller area network (CAN) – Part 1: Data link layer and physical signalling.* ISO, Geneva, Switzerland.

H.S. Bae, J. Ruy, and J. Gerdes. 2001. Road grade and vehicle parameter estimation for longitudinal control using GPS. In *Proceedings of IEEE Conference on Intelligent Transportation Systems*, San Francisco, CA.

R. Brüntrup, S. Edelkamp, S. Jabbar, and B. Scholz. 2005. Incremental map generation with GPS traces. In *Proceedings of IEEE Intelligent Transportation Systems*, Vienna, Austria.

A. Carlsson, G. Baumann, and H.C. Reuss. 2008. Implementation of a self-learning route memory as an electronic co-driver for reduced emissions. In *FISITA World Automotive Congress*, Munich, Germany.

A. El-Rabbany. 2006. *Introduction to GPS : the global positioning system*, 2. ed. edition. Artech House, Boston. ISBN 1-59693-016-0.

H.K. Fathy, D. Kang, and J.L. Stein. 2008. Online vehicle mass estimation using recursive least squares and supervisory data extraction. In *Proceedings of American Control Conference*, Seattle, Washington, USA.

Anders Fröberg. 2008. *Efficient Simulation and Optimal Control for Vehicle Propulsion.* PhD thesis, Linköpings universitet.

E.G. Gaeke. 1973. Road grade sensor. US Patent #3,752,251. Filing date: Aug 17, 1971 Issue date: Aug 1973 Inventor: Edward G. Gaeke Assignee: General Motors Corporation.

J.D. Gonder. 2008. Route-based control of hybrid electric vehicles. In *SAE World Congress & Exhibition, April 2008*, Detroit, MI, USA. 2008-01-1315.

F. Gustafsson. 2000. *Adaptive filtering and change detection.* John Wiley & Sons, LTD, Chichester.

S. Han and C. Rizos. 1999. Road slope information from gps-derived trajectory data. *Journal of Surveying Engineering*, 125(2):59–68.

E. Hellström. 2007. Look-ahead control of heavy trucks utilizing road topography. Licentiate thesis, Linköpings universitet. LiU-TEK-LIC-2007:28, Thesis No. 1319.

E. Hellström, M. Ivarsson, J. Åslund, and L. Nielsen. 2007. Look-ahead control for heavy trucks to minimize trip time and fuel consumption. In *Fifth IFAC Symposium on Advances in Automotive Control*, Monterey Coast CA, USA.

S. Ichikawa, Y. Yokoi, S. Doki, S. Okuma, T. Naitou, T. Shiimado, and N. Miki. 2004. Novel energy management system for hybrid electric vehicles utilizing car navigation over a commuting route. In *Intelligent Vehicles Symposium, 2004 IEEE*, pages 161–166.

L. Johannesson. 2006. On energy management strategies for hybrid electric vehicles. Licentiate thesis, Chalmers tekniska högskola. Series: R - Department of Signals and Systems, Chalmers University of Technology, no: R022.

L. Johannesson and B. Egardt. 2007. A novel algorithm for predictive control of parallel hybrid powertrains based on dynamic programming. In *Fifth IFAC Symposium on Advances in Automotive Control*, Monterey Coast CA, USA.

U. Kiencke and L. Nielsen. 2003. *Automotive Control Systems*. Springer Verlag, Berlin.

J.P. Lauffenburger, B. Bradai, A. Herbin, and M. Basset. 2007. Navigation as a virtual sensor for enhanced lighting preview control. In *IEEE Intelligent Vehicles Symposium*.

P. Lingman and B. Schmidtbauer. 2001. Road slope and vehicle mass estimation using Kalman filtering. In *Proceedings of the 17th IAVSD Symposium*, Copenhagen, Denmark.

J. Löwenau, K. Gresser, D. Wisselmann, W. Richter, D. Raber, and S. Durekovic. 2006. *Advanced Microsystems for Automotive Applications 2006*, chapter Dynamic Pass Prediction - A New Driver Assistance System for Superior and Safe Overtaking, pages 67–77. Springer-Verlag, Berlin, Germany.

J. Löwenau, P.J.Th. Venhovens, and J.H. Bernasch. 2000. Advanced vehicle navigation applied in the bmw real time light simulation. *The Journal of Navigation*, 53:30–41.

P. Misra and P. Enge. 2006. *Global positioning system : signals, measurements and performance*, 2. ed. edition. Ganga-Jamuna Press, Lincoln, Mass. ISBN 0-9709544-1-7.

NAVTEQ Press Release, 2008. *NAVTEQ Announces Industry Strategy for Map- Enhanced Advanced Driver Assistance Systems*. NAVTEQ, 425 West Randolph Street, Chicago, Illinois 60606, USA. URL `http:`

//www.navteq.com/webapps/NewsUserServlet?action=NewsDetail&newsId=666&lang=en&englishonly=false. 4 Nov. 2008.

U. Noyer, H. Mosebach, S. Karrenberg, H. Philipps, J. Rataj, and A. Bartels. 2008. Modeling freeways for digital high precision maps. In *FISITA World Automotive Congress*, Munich, Germany.

Oxford Technical Solutions Limited, 2008. *User Manual; Covers RT2000, RT3000 and RT4000 products*. Oxford Technical Solutions Limited, 77 Heyford Park, Upper Heyford, Oxfordshire, OX25 5HD, England. URL http://www.oxts.co.uk/downloads/rtman.pdf. 4 Nov. 2008.

N. Pettersson and K.H. Johansson. 2006. Modelling and control of auxiliary loads in heavy vehicles. *International Journal of Control*, 79(5):479 – 95. ISSN 0020-7179.

Racelogic Limited, 2008. *VBOX III 100Hz GPS Data Logger User Guide*. Racelogic Limited, Unit 10, Swan Business Centre, Osier Way, Buckingham MK18 1TB, United Kingdom. URL http://www.racelogic.co.uk/_downloads/vbox/Manuals/Data_Loggers/RLVB3_Manual\%20-\%20English.pdf. 4 Nov. 2008.

H.E. Rauch, F. Tung, and C.T. Striebel. 1965. Maximum likelihood estimates of linear dynamic systems. *AIAA Journal*, 3(8):1445 – 1450.

C. Ress, D. Balzer, A. Bracht, S. Durekovic, and J. Löwenau. 2008. Adasis protocol for advanced in-vehicle applications. In *15th World Congress on Intelligent Transport Systems*, New York, NY, USA.

P. Sahlholm. 2008. Improved heavy duty vehicle performance through the use of 3d map data. In *15th World Congress on Intelligent Transport Systems*, New York, NY, USA.

P. Sahlholm, H. Jansson, and K.H. Johansson. 2007a. Road grade estimation results using sensor and data fusion. In *14th World Congress on Intelligent Transport Systems*, Beijing, China.

P. Sahlholm, H. Jansson, and K.H. Johansson. 2008. Road grade estimation for look-ahead vehicle control. In *17th IFAC World Congress*, Seoul, Korea.

P. Sahlholm, H. Jansson, E. Kozica, and K.H. Johansson. 2007b. A sensor and data fusion algorithm for road grade estimation. In *Fifth IFAC Symposium on Advances in Automotive Control*, Monterey Coast CA, USA.

F.R. Salmasi. 2007. Control strategies for hybrid electric vehicles: Evolution, classification, comparison, and future trends. *Vehicular Technology, IEEE Transactions on*, 56(5):2393–2404. ISSN 0018-9545.

S. Schroedl, K. Wagstaff, S. Rogers, P. Langley, and C. Wilson. 2004. Mining gps traces for map refinement. *Data Mining and Knowledge Discovery*, 9:59–87.

S. Terwen, M. Back, and V. Krebs. 2004. Predictive powertrain control for heavy duty trucks. In *Proceedings of IFAC Symposium on Advances in Automotive Control*, Salerno, Italy.

Swedish Road Authorities, 2004. *Vägars och gators utformning, VGU*, 2004:80 edition. Vägverket, Sektion Utformning av vägar och gator, Vägverket, Butiken, SE-781 87 Borlänge, Sweden.

A. Vahidi, A. Stefanopolou, and H. Peng. 2005. Recursive least squares with forgetting for online estimation of vehicle mass and road grade: Theory and experiments. *Journal of Vehicle System Dynamics*, 43:31–57.

Vector Informatik, 2008. *Hardware Interfaces for CAN and LIN*. Vector Informatik GmbH, Ingersheimer Str. 24, D-70499 Stuttgart, Germany. URL `http://www.vector-worldwide.com/portal/medien/cmc/datasheets/CAN_LIN_Interfaces_DataSheet_EN.pdf`. 4 Nov. 2008.